The *Arabidopsis* Glucosyltransferase UGT76B1 Conjugates Isoleucic Acid and Modulates Plant Defense and Senescence [C][W][OA]

Veronica von Saint Paul,[a] Wei Zhang,[a] Basem Kanawati,[b] Birgit Geist,[a] Theresa Faus-Keßler,[c] Philippe Schmitt-Kopplin,[b] and Anton R. Schäffner[a],[1]

[a] Institute of Biochemical Plant Pathology, Helmholtz Zentrum München, 85764 Neuherberg, Germany
[b] Institute of Ecological Chemistry, Helmholtz Zentrum München, 85764 Neuherberg, Germany
[c] Institute of Developmental Genetics, Helmholtz Zentrum München, 85764 Neuherberg, Germany

Plants coordinate and tightly regulate pathogen defense by the mostly antagonistic salicylate (SA)- and jasmonate (JA)-mediated signaling pathways. Here, we show that the previously uncharacterized glucosyltransferase UGT76B1 is a novel player in this SA-JA signaling crosstalk. *UGT76B1* was selected as the top stress-induced isoform among all 122 members of the *Arabidopsis thaliana UGT* family. Loss of *UGT76B1* function leads to enhanced resistance to the biotrophic pathogen *Pseudomonas syringae* and accelerated senescence but increased susceptibility toward necrotrophic *Alternaria brassicicola*. This is accompanied by constitutively elevated SA levels and SA-related marker gene expression, whereas JA-dependent markers are repressed. Conversely, *UGT76B1* overexpression has the opposite effect. Thus, *UGT76B1* attenuates SA-dependent plant defense in the absence of infection, promotes the JA response, and delays senescence. The *ugt76b1* phenotypes were SA dependent, whereas *UGT76B1* overexpression indicated that this gene possibly also has a direct effect on the JA pathway. Nontargeted metabolomic analysis of *UGT76B1* knockout and overexpression lines using ultra-high-resolution mass spectrometry and activity assays with the recombinant enzyme led to the ab initio identification of isoleucic acid (2-hydroxy-3-methyl-pentanoic acid) as a substrate of UGT76B1. Exogenously applied isoleucic acid increased resistance against *P. syringae* infection. These findings indicate a novel link between amino acid–related molecules and plant defense that is mediated by small-molecule glucosylation.

INTRODUCTION

Plants are sessile organisms and cannot escape adverse environmental cues. Therefore, they have evolved elaborate mechanisms to antagonize these stresses and to organize defense or tolerance. These measures involve a complex reprogramming of plant cells, which relies on major changes in gene expression, protein modification, and a range of different compounds active in defense and signaling. Several small-molecule hormones, such as salicylic acid (SA), jasmonic acid (JA), ethylene, and abscisic acid play crucial roles in regulating responses of plants to both biotic and abiotic stresses. These signaling pathways interact with each other in synergistic as well as antagonistic manners, enabling the plant to fine-tune its response to the stressor(s) encountered (Jones and Dangl, 2006; Koornneef and Pieterse, 2008). Constitutive production of signaling molecules

and the concomitant expression of defense genes is energetically costly, and reallocation of resources toward defense seems to decrease plant overall fitness (Heil and Baldwin, 2002; Lorrain et al., 2003). Therefore, plants need a tight control of the defense response and its suppression in the absence of pathogen attack or other stresses (Heidel et al., 2004; Bolton, 2009). Mostly, SA- and JA-mediated signaling pathways are triggered when plants defend themselves against pathogens. Although concerted actions of both pathways have been reported, they usually act in an antagonistic manner via mutual repression (Glazebrook, 2005; Jones and Dangl, 2006; Spoel et al., 2007; Koornneef et al., 2008; Vlot et al., 2009). Whereas biotrophic pathogens (bacteria, fungi, and viruses) are mostly combatted by the SA pathway, the opposite prioritization of defense signaling is mobilized to fight necrotrophic pathogens (bacteria and fungi) and herbivores.

Arabidopsis thaliana genetics has defined a plethora of genes involved in both SA and JA signaling and their interplay. A number of mutants resulted in enhanced susceptibility to biotrophic pathogens and suppression of SA responses and could therefore be used to define the crucial steps in SA signaling. These include components of the mitogen-activated protein kinase signaling pathway, such as ERD1, MPK3, and MPK6; genes related to SA biosynthesis, such as *ICS1/SID2*, *PAD4*, and *EDS1*; central downstream regulators of SA signaling, such as *NPR1*; as well as WRKY and TGA transcription factors.

Induction of these transcription factors eventually leads to the activation of SA-responsive genes, including *PR* genes that are involved in defense responses. Similarly, mutations in genes such as *JAR1*, *COI1*, and *JIN1*, which define different steps in JA signaling, negatively affect the JA pathway (Kazan and Manners, 2008). Resistance toward necrotrophic pathogens is reduced in the corresponding mutants concomitant with the abolished induction of marker genes, like the defensin *PDF1.2*. By contrast, several gain-of-resistance *Arabidopsis* mutants, such as *mlo*, *mpk4*, *wrky*, *acd*, *lsd*, *hrl1*, *hlm1*, or *dnd*, show constitutive defense responses in the absence of (biotrophic) pathogen attack, which affects pathogen perception and response or leads to primed defense (Greenberg et al., 1994; Petersen et al., 2000; Devadas et al., 2002; Balagué et al., 2003; Lorrain et al., 2003; Consonni et al., 2006; Journot-Catalino et al., 2006; Genger et al., 2008). Other interesting classes of mutants with enhanced resistance affecting various steps in signal transduction are the *cpr* mutants, named after the *CONSTITUTIVE ACTIVATION OF PR* genes, and several suppressors of *npr1* mutants, such as *ssi* and *sni*. These mutants are usually characterized by transcriptional activation of *PR* genes and constitutive accumulation of SA (Bowling et al., 1994; Li et al., 1999; Shah et al., 1999; Gou et al., 2009). In addition, several of the mutants resistant to biotrophic pathogens exhibit retarded growth and/or accelerated senescence. Notably, developmental senescence is at least in part regulated by an SA-dependent pathway (Buchanan-Wollaston et al., 2005).

It has been shown that some of the genes mentioned above (such as those encoding MPK4, WRKY transcription factors, and NPR1) exert opposite effects on the SA and JA pathways. Thus, they are integral to the SA-JA crosstalk (Koornneef and Pieterse, 2008; Vlot et al., 2009). Interestingly, two aminotransferase mutants, *agd2* and *ald1*, have an opposite influence on pathogen susceptibility, which points toward a possible involvement of amino acid–related molecules in the regulation of defense (Song et al., 2004). Although the existence of several SA and JA amino acid conjugates is known, the direct involvement of amino acids in defense has been shown only in the case of JA-Ile, which is the major, bioactive form of jasmonate (Staswick and Tiryaki, 2004; Fonseca et al., 2009).

Plant secondary metabolite UDP-dependent glycosyltransferases (UGTs) catalyze the transfer of a carbohydrate from an activated donor sugar onto small molecule acceptors by the formation of a glycosidic bond (Mackenzie et al., 1997; Li et al., 2001). Glycosylation changes the stability and/or solubility of the aglyca, and it may even create a higher diversity due to differential and multiple conjugations. These reactions are an important feature of the biosynthesis of many secondary metabolites and in many cases of the regulation of the activity of signaling molecules and defense compounds. They may include detoxification and compartmentation of endogenous compounds and xenobiotics (Jones and Vogt, 2001). One hundred and twenty-two different UGT isoforms exist in *Arabidopsis*, which represent 0.5% of all annotated genes in this species (Ross et al., 2001; Bowles et al., 2005; Gachon et al., 2005). Analyses of recombinant UGT proteins led to the identification of UGTs with in vitro activity toward several endogenous compounds, like auxin (Jackson et al., 2001), abscisic acid (Lim et al., 2005), flavonoids

(Jones et al., 2003), lignin precursors, hydroxybenzoic acids (Lim et al., 2002), and thiohydroximate (Grubb et al., 2004), as well as toward xenobiotics (Messner et al., 2003; Brazier-Hicks and Edwards, 2005). However, these activities could be confirmed in vivo only in a few cases, possibly due to the broad substrate acceptance of some UGT enzymes in vitro or to a limited substrate availability in vivo (Jones and Vogt, 2001; Gachon et al., 2005; Bowles et al., 2006). So far, there is in vivo evidence that flavonoids, SA, indole-3-acetic acid, glucosinolates, and brassinosteroids function as endogenous substrates of UGT enzymes in *Arabidopsis* (Jackson et al., 2002; Grubb et al., 2004; Poppenberger et al., 2005; Tohge et al., 2005; Dean and Delaney, 2008; Song et al., 2008; Yonekura-Sakakibara et al., 2008). The substrates of the vast majority of UGT isoforms, however, have not been identified, and these isoforms thus remain orphan glycosyltransferases. An approach to gauge the impact of UGTs on plant defense irrespective of the knowledge of their substrates was also undertaken. The expression of various candidate *UGT* genes was altered (e.g., *ugt73b3* and *ugt73b5* knockout mutants were generated; *UGT74F2* was overexpressed), and a decrease in resistance to pathogen infection indicated a role for these isoforms in defense (Langlois-Meurinne et al., 2005; Song et al., 2008).

In this project, we scanned public expression databases for stress-responsiveness of *UGT* genes and found that the otherwise uncharacterized *UGT76B1* was the member of this family that exhibited the greatest induction in response to stress. *UGT76B1* was broadly upregulated by both abiotic and biotic cues. Furthermore, it was one of only three *UGT* genes (with *UGT72B1* and *UGT75B1*) that was induced by both SA and JA (methyl jasmonate) application. *ugt76b1* knockout lines exhibited enhanced resistance toward *Pseudomonas syringae* infection, yet higher susceptibility toward necrotrophic *Alternaria brassicicola*, and they progressed earlier into senescence. By contrast, *UGT76B1* overexpression resulted in the opposite phenotypes. Using a nontargeted metabolomic approach based on ultra-high-resolution Fourier transform ion cyclotron resonance mass spectrometry (FT-ICR MS), we could pinpoint isoleucic acid (ILA) as an endogenous substrate of UGT76B1. Exogenously applied ILA itself activated SA-dependent marker gene expression and enhanced resistance toward infection with avirulent *P. syringae*. Collectively, these findings indicate that UGT76B1 and ILA are novel players in SA- and JA-mediated responses. UGT76B1 acts as a negative regulator of SA-dependent plant defense in the absence of pathogens, promotes the JA response, and negatively influences the onset of senescence.

RESULTS

A Subset of Genes Accounts for the Majority of Stress-Dependent Transcriptional Inductions within the *UGT* Family

To analyze the distribution of transcriptional responses to exogenous stresses within the *Arabidopsis UGT* genes, we examined public expression data of plants exposed to several abiotic and biotic stress cues. A total of 112 probe sets on the ATH1

microarray represent 105 *UGT* genes by gene-specific probes, while seven hybridize to two highly related genes each. Normalized expression data from Columbia (Col) wild-type leaves or seedlings were retrieved from the BAR database (bbc.botany. utoronto.ca; Toufighi et al., 2005). A large group of *UGT* genes was induced in one or several experiments, but stress responsiveness was not equally distributed across the genes analyzed. In both abiotic and biotic stress experiments, a clear clustering of stress-dependent induction was observed (Figure 1; see Methods). *UGT76B1* was the top stress-induced *UGT*, being highly responsive to abiotic cues such as UV-B irradiation, osmotic, oxidative, drought, or wounding stresses as well as to both biotrophic and necrotrophic pathogens. Since the *UGT76B* subfamily only contains this unique member, *UGT76B1* may have an important and specific role in plant stress responses.

ugt76b1 Knockout and *UGT76B1* Overexpression Lines

To study whether *UGT76B1* has any function in plant stress responses and to determine how this might affect the plant, we obtained *Arabidopsis* loss-of-function mutants and generated constitutive overexpression lines of *UGT76B1*. Two T-DNA insertion lines, SAIL_1171A11 and GT_5_11976, in two different genetic backgrounds (Col-0 and Landsberg erecta [L*er*]) were characterized as *ugt76b1-1* and *ugt76b1-2* knockout mutants, respectively (see Methods; see Supplemental Figure 1 online). *Arabidopsis* lines overexpressing *UGT76B1* under the control of 35S-derived constitutive promoters were generated, and two homozygous lines with single insertions were selected (see Methods). Both lines, *UGT76B1-OE-5* and *UGT76B1-OE-7*, showed a significantly higher transcript level compared with the wild type (see Supplemental Figure 1 online).

UGT76B1 Expression Affects Onset of Senescence

UGT76B1-OE-7 and *ugt76b1* knockout lines were examined for morphological or developmental phenotypes associated with a change in *UGT76B1* expression. All genotypes germinated at the same time. No obvious morphological differences were found in lines with altered *UGT76B1* expression compared with the wild type, except for a tendency for smaller rosettes of the *ugt76b1* knockout lines and for enlarged rosettes in the case of *UGT76B1-OE-7* (see Supplemental Figure 2 online). However, mutant and overexpression lines showed a clearly altered onset of developmental as well as dark-induced senescence. The knockout plants developed yellowing of leaves 6 weeks after germination, while the wild type did not yet show any signs of senescence (Figure 2A; see Supplemental Figure 3A online). After 9 weeks, *ugt76b1-1* was completely senescent, the wild type only started to show the first signs of leaf yellowing, and the overexpression line still showed mostly dark-green leaves (Figure 2B).

Similar visible differences were found when we analyzed dark-induced senescence in detached leaves (Figure 2C; see Supplemental Figure 3B online).

To confirm that the leaf yellowing of *ugt76b1-1* is due to an accelerated onset of developmentally induced senescence, we monitored the expression of two marker genes. *SAG13* is induced during early senescence, whereas *SAG12* is specifically activated during the later stages of developmentally regulated senescence, when the leaves start to show yellowing (Weaver et al., 1998). Both senescence marker genes *SAG12* and *SAG13* were more strongly induced in *ugt76b1-1* knockout plants than in the wild type, whereas expression was much lower in *UGT76B1-OE-7* (Figure 2D).

UGT76B1 Overexpression and Loss of Function Alter Pathogen Susceptibility in an Opposite Manner

As changing *UGT76B1* expression had no influence on plant resistance to abiotic stressors like UV irradiation and salt, we tested whether alterations in *UGT76B1* expression would affect the susceptibility of the plant to biotrophic pathogens. Whole leaves of *ugt76b1-1*, *UGT76B1-OE-7*, and Col-0 were inoculated with 5×10^5 colony-forming units (cfu) mL^{-1} avirulent *P. syringae* strain D3000 *AvrRpt2* (*Ps-avir*). The bacteria showed the typical proliferation of *Ps-avir* in Col-0 30 and 78 h after inoculation. In the knockout plant, nearly no bacterial growth was observed, pointing to a significantly reduced susceptibility, whereas in the overexpression line, the bacterial population strongly increased, indicating a reduced resistance (Figure 3A). The second knockout line, *ugt76b1-2*, showed the same pathogen resistance–related phenotype (see Supplemental Figure 3C online). Similar results were obtained with virulent *P. syringae* DC3000 (*Ps-vir*, Figure 3). In both cases, *UGT76B1* expression negatively correlated with plant resistance to the biotrophic pathogen *P. syringae*.

We also analyzed the susceptibility of mutant and overexpression lines toward the necrotrophic fungus *A. brassicicola*. Here, exactly the opposite effect was observed: *ugt76b1-1* was less resistant to infection, whereas *UGT76B1* overexpression led to enhanced resistance (Figure 3B). Thus, *UGT76B1* expression directly correlated with resistance against the necrotrophic infection.

Defense Marker Gene Expression Is Constitutively Altered in *UGT76B1-OE* and *ugt76b1* Lines

Since the differential effects of *UGT76B1* overexpression and loss of function on either biotrophic or necrotrophic pathogen infections pointed to an altered plant defense in these lines, we analyzed several marker genes diagnostic for the antagonistic SA- and JA-dependent pathways using relative quantification by real-time quantitative RT-PCR (qRT-PCR). *PAD4* and *EDS1* act upstream from SA biosynthesis but are also induced by SA (Rustérucci et al., 2001). *PR1* is a pathogen- and SA-responsive gene, which is a well-established marker gene for the defense responses of *Arabidopsis* against *P. syringae* (Uknes et al., 1992). *SAG13* is an early senescence marker, which is also induced by several stress factors and SA (Weaver et al., 1998). *WRKY70* encodes a transcription factor and is an important regulator in the interplay of SA- and JA-related plant defense responses (Li et al., 2004). *PDF1.2* and *VSP2* are marker genes frequently used to monitor JA responses (Pieterse et al., 2009), whereas *LOX2*, which is involved in JA biosynthesis, is activated by a positive feedback loop (Sasaki et al., 2001).

Changing *UGT76B1* expression had a strong effect on the transcript level of these defense-related genes (Figure 4A). *PR1*,
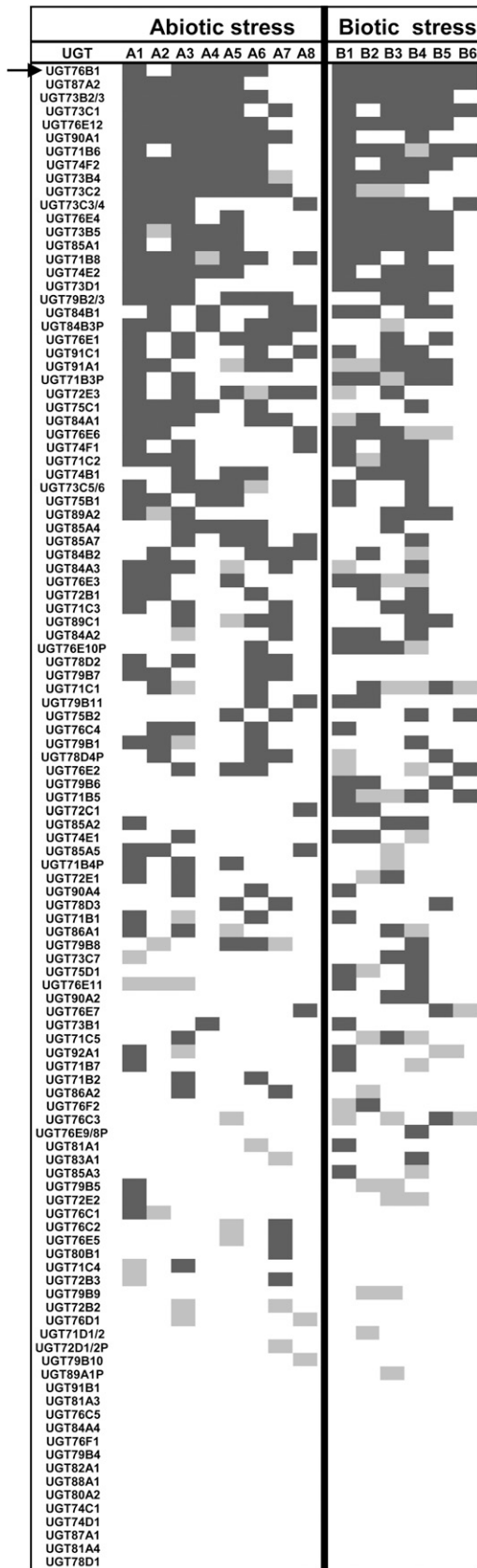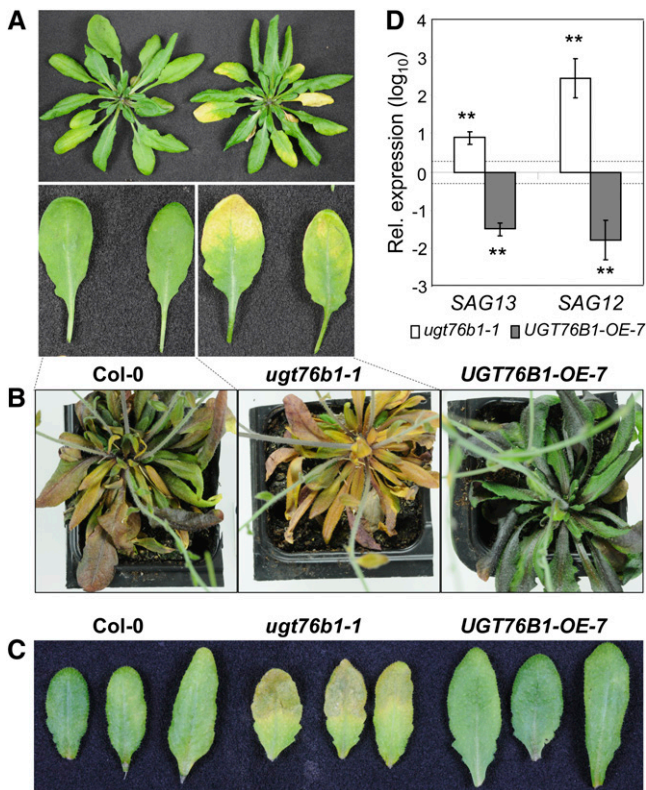
PAD4, *EDS1*, *WRKY70*, and *SAG13* were induced in leaves of 5-week-old untreated *ugt76b1* knockout plants compared with the wild type. By contrast, JA-responsive genes *PDF1.2* and *VSP2* as well as *LOX2* were downregulated. *UGT76B1-OE-7* showed the opposite regulation for all measured genes. *PR1*, *PAD4*, *EDS1*, *WRKY70*, and *SAG13* were downregulated, whereas *VSP2* and *LOX2* were upregulated. The upregulation of *PDF1.2* in *UGT76B1-OE-7* was more variable in different experiments. To exclude an age-dependent effect on *PR1* expression (Kus et al., 2002), *PR1* and *SAG13* were analyzed also in 3-week-old plants. Again, both genes showed a similar, opposite regulation in knockout and overexpression lines (see Supplemental Figure 4 online).

To analyze whether the overexpression line was still able to induce SA-dependent defense after *P. syringae* challenge, although it was compromised by the strong constitutive repression of this pathway, we quantified the transcription of *PR1* and *SAG13* in wild-type, mutant, and *UGT76B1*-overexpressing plants after bacterial inoculation. In wild-type plants, *PR1* and *SAG13* were induced 24 h after infection with *Ps-avir* to similar levels as those constitutively expressed in the *ugt76b1* loss-of-function mutant. In the overexpression line, transcripts of both *PR1* and *SAG13* reached similar levels as in wild-type plants 24 h after pathogen challenge. Thus, the potential to perceive the pathogen and eventually activate the SA signaling pathway was retained in the *UGT76B1* overexpression line.

Endogenous Levels of Free and Conjugated SA Are Elevated in *ugt76b1*

EDS1 and *PAD4* are essential regulators of basal resistance and are known to regulate the accumulation of the signaling molecule SA (Zhou et al., 1998; Rustérucci et al., 2001). In addition, several mutants with constitutive transcriptional activation of *PR* genes are known to have increased levels of SA and its glucosides (Silva et al., 1999; Balagué et al., 2003; Gou et al., 2009). We therefore assessed whether the high level of *PR1* expression in *ugt76b1-1* plants was correlated with higher endogenous SA levels (Figure 5). Indeed, *ugt76b1-1* showed a considerably higher basal level of SA and its glucosides than wild-type plants in the absence of any inducer. By contrast, the overexpression line contained a slightly repressed, yet not significantly altered, amount of free SA compared with wild-type plants but also higher levels of the SA

Figure 1. Stress-Responsive Expression of *UGT* Genes in *Arabidopsis* Leaves and Seedlings Based on Affymetrix ATH1 Microarray Data.

The distribution of maximal inductions to abiotic and biotic stress factors among all *UGT* members is shown. Significant inductions equal or higher than twofold (dark gray) and higher than 1.5-fold (light gray) are indicated. Genes are sorted from highest to lowest abiotic and biotic stress inducibility using mutual ranking (see Methods). The top stress-induced gene, *UGT76B1*, which was used for further analysis, is indicated with an arrow. A1, osmotic; A2, salt; A3, UV-B; A4, oxidative; A5, wounding; A6, drought; A7, cold; A8, heat; B1, *P. syringae* pv *tomato* DC3000 (virulent); B2, *P. syringae* pv *phaseolicula* (avirulent); B3, *Phytophthora infestans*; B4, *Botrytis cinerea*; B5, P. *syringae* pv *maculicola* ES4326 (virulent); B6, *Erysiphe orontii*.

Figure 2. Senescence Phenotypes of *ugt76b1* Knockout and *UGT76B1* Overexpression Lines.

(A) Natural senescence in 6.5-week-old Col-0 and *ugt76b1-1* mutant plants.

(B) Natural senescence in 9-week-old Col-0, *ugt76b1-1*, and *UGT76B1-OE-7* plants.

(C) Dark-induced senescence in Col-0, *ugt76b1-1*, and *UGT76B1-OE-7* plants. Excised leaves from 5-week-old plants were kept in water and darkness for 5 d. The second knockout line, *ugt76b1-2*, showed the same senescence-related phenotype (see Supplemental Figures 3A and 3B online).

(D) Relative quantification of senescence-associated marker genes *SAG13* and *SAG12* in 7-week-old wild-type, *ugt76b1-1*, and *UGT76B1-OE-7* plants (leaves 7 to 9). Transcript levels were normalized to *UBIQUITIN5* and *S16* transcripts; levels relative to Col-0 plants are displayed. Arithmetic means and standard errors from $\log_{10}$-transformed data of two experiments (each based on three independent replicates) were calculated. Asterisks indicate significance of the difference to the wild-type line; **P value < 0.01. The dashed lines indicate a twofold change.

conjugates. The SA ester level did not significantly change in overexpression lines but was slightly increased in the knockout mutant (Figure 5).

Dependence of UGT76B1-Related Responses on SA and JA Pathways

UGT76B1 overexpression and loss of function antagonistically affected SA- and JA-dependent responses. To analyze how these responses were integrated into the corresponding path-

ways, *ugt76b1-1* and *UGT76B1-OE-7* were introgressed in *sid2* and *NahG* as well as in *jar1* lines. *SID2* is responsible for stress-induced SA biosynthesis; consequently, its loss of function leads to an impaired SA-dependent defense (Nawrath and Métraux, 1999). The *NahG* line, by contrast, leads to an almost complete loss of SA, including basal levels, due to the hydrolytic activity of
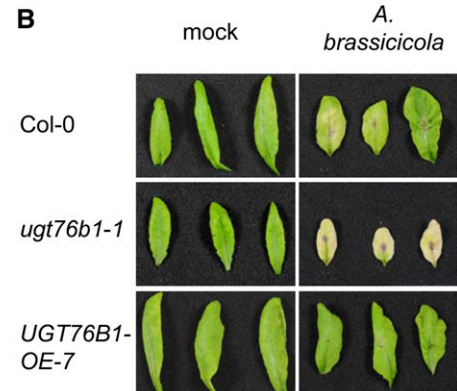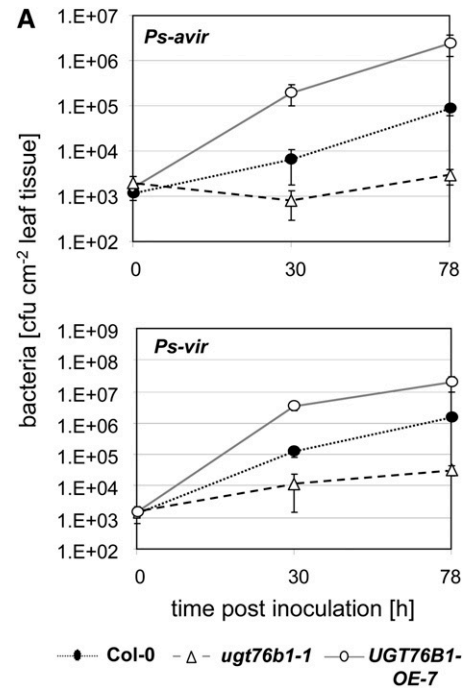
Figure 3. Pathogen Susceptibility Is Affected in Opposite Directions in *UGT76B1* Overexpression and Loss-of Function Lines.

(A) Bacterial growth of avirulent (*avir*) and virulent (*vir*) *P. syringae* (*Ps*) in *Arabidopsis* leaves of wild-type, *ugt76b1-1*, and *UGT76B1-OE-7* plants. Leaves were infiltrated with an inoculum of 5×10^5 cfu mL^{-1} of *Ps-avir* (top graph) and *Ps-vir* (bottom graph). Bacteria (cfu cm^{-2}) were quantified 30 and 78 h after inoculation. The graphs represent the means and standard deviations of three replicates.

(B) Enhanced/decreased resistance of *UGT76B1-OE-7*/*ugt76b1-1* lines to *A. brassicicola*. Four-week-old plants were infected with 7.5×10^3 spores (see Methods). Photographs were taken 2 weeks after infection. The experiments were repeated with similar results.
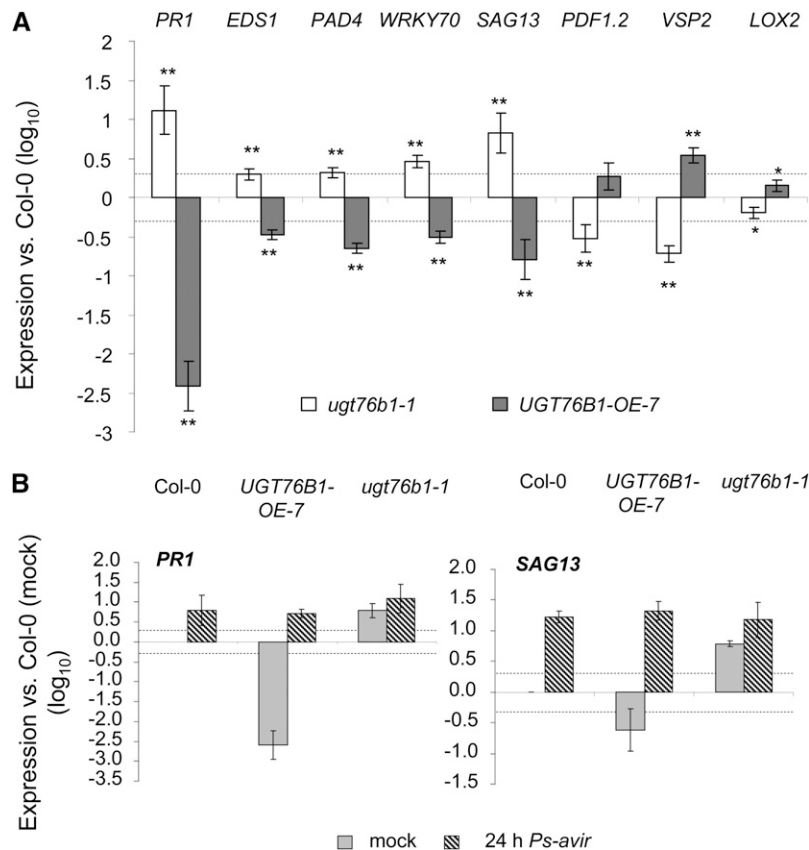
Figure 4. Defense Marker Gene Expression in *ugt76b1-1* and *UGT76B1-OE-7* Plants before and after Pathogen Infection.

(A) Gene expression of *PR1*, *EDS1*, *PAD4*, *WRKY70*, *SAG13*, *PDF1.2*, *VSP2*, and *LOX2* in 5-week-old *ugt76b1-1* and *UGT76B1-OE-7* measured by qRT-PCR. Expression levels were normalized to *UBIQUITIN5* and *S16* transcripts; levels relative to Col-0 plants are displayed. Arithmetic means and standard errors from $\log_{10}$-transformed data of two experiments each consisting of three independent replicates were calculated using ANOVA. Asterisks indicate significance of the difference to the wild-type line; **P value < 0.01 and *P value < 0.05.

(B) Transcript levels of *PR1* and *SAG13* in 5-week-old wild-type plants 24 h after infection (5×10^5 cfu mL^{-1} *Ps-avir*) measured by qRT-PCR. Values are relative to expression 24 h after mock treatment and $\log_{10}$ transformed. Bars represent the mean and standard deviation of three replicates. The dashed, horizontal lines indicate a twofold change.

the bacterial transgene *NahG* (Gaffney et al., 1993). On the other hand, loss of *JAR1* blocks the JA pathway at the formation of the bioactive JA-Ile conjugate (Staswick and Tiryaki, 2004).

The *ugt76b1*-dependent induction of the SA marker genes *PR1* and *SAG13* was reverted (or at least eliminated) after introgression into the *sid2* and *NahG* backgrounds, indicating its dependence on SA in both cases (Figure 6A). However, *PR1*, and, to a lesser extent, *SAG13* were still significantly increased in *ugt76b1 sid2* compared with *sid2*, similar to their induction in *ugt76b1-1* compared with the wild type. Thus, the *ugt76b1*-dependent activation was at least partially functional in the *sid2* background, which still contains basal SA levels. However, the activation completely relied on total SA levels, since in *ugt76b1 NahG* plants, *PR1* and *SAG13* were fully suppressed like in the *NahG* line alone (Figure 6A). The early senescence phenotype as well as the reduced rosette size of *ugt76b1-1* was completely abolished by *sid2*, in agreement with the expression of the marker gene *SAG13*, which was identical for the wild type and

ugt76b1 sid2. Lack of *JAR1* did not influence these phenotypes (Figure 6B; see Supplemental Figure 5 online).

The *ugt76b1*-dependent suppression of the JA marker *VSP2* was fully dependent on both *SID2*-related and total SA levels, since in both *ugt76b1 sid2* and *ugt76b1 NahG* the expression of *VSP2* was reverted to the level of the *sid2* and *NahG* lines, respectively (Figure 6A).

The combination of *UGT76B1-OE-7* and *sid2* indicated that the transcriptional effects of the ectopic expression of *UGT76B1* did not rely on the suppression of *SID2*. *VSP2* induction in relation to the wild type was basically unchanged with and without introgression of *sid2* and also significant in *UGT76B1-OE sid2* with respect to *sid2* alone. The *UGT76B1-OE*–dependent suppression of *PR1* and *SAG13* was also retained in the *sid2* background (Figure 6A).

The induction and repression of *PR1* and *SAG13* in *ugt76b1-1* and *UGT76B1-OE-7*, respectively, were maintained after crossing both lines with *jar1* and were thus independent from the
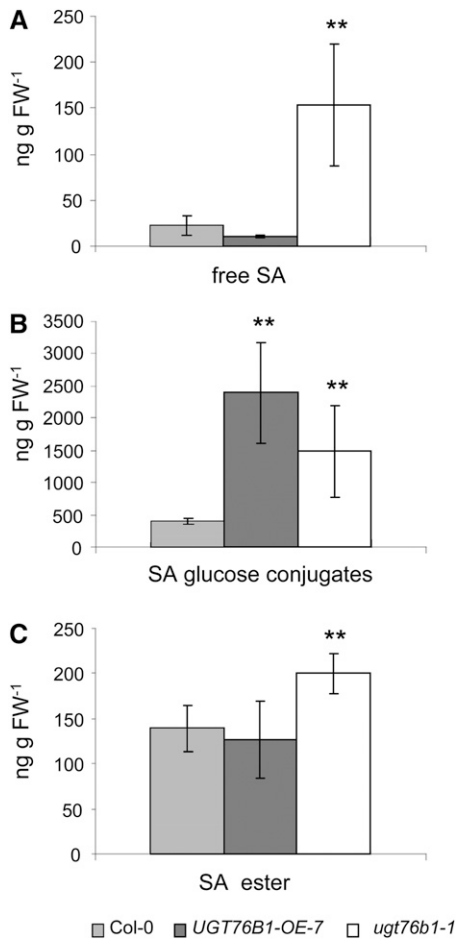
Figure 5. SA and Conjugated SA Levels in 5-Week-Old Seedlings of the Wild Type, *ugt76b1-1*, and *UGT76B1-OE-7*.

Values represent the means and standard deviations obtained from five replicates. Asterisks indicate significance of the difference to the wild-type line; **P value < 0.01. The experiment was repeated with similar results. Free SA **(A)**, SA Glc conjugates **(B)**, and SA ester **(C)**. FW, fresh weight.

related formation of JA-Ile. On the other hand, *VSP2* induction in the overexpression line, which was not affected by *sid2* (see above), was abolished by the introgression of *jar1* (Figure 6B). Therefore, ectopic *UGT76B1* expression acted in a *JAR1*-dependent, but *SID2*-independent, manner to activate the JA pathway. Nevertheless, *UGT76B1* overexpression was able to revert the reduced growth phenotype of *jar1* plants (see Supplemental Figure 5 online).

UGT76B1 Is Induced Early after Pathogen Infection before *PR1*

To determine at which time point after pathogen infection *UGT76B1* transcription was activated, we analyzed the kinetics of *UGT76B1* expression after pathogen infection compared with other defense marker genes known to be induced at early or late phases during the defense response. Figure 7 shows the time course of *UGT76B1*, *SAG13*, *WRKY70*, *EDS1*, *PAD4*, and *PR1*

expression during the incompatible interaction of wild-type plants with *Ps-avir*. *PR1* and *SAG13* were highly induced 24 h after pathogen inoculation. *UGT76B1* as well as *WRKY70*, *EDS1*, and *PAD4* preceded the upregulation of *PR1* and *SAG13*.

### Spatial Expression Pattern of *UGT76B1*

To analyze the expression of *UGT76B1* in different plant organs and at different developmental stages, transgenic lines carrying a *UGT76B1*_{pro}:*GFP-GUS* (for green fluorescent protein and β-glucuronidase) construct were produced (see Methods). Plants in different developmental stages (8, 17, 28, and 36 d) showed consistent GUS activity among two independent transgenic lines. *UGT76B1* was expressed throughout the roots, except in root tips. Stronger expression was found in young roots and in lateral roots (Figures 8A and 8D). Confocal laser scanning microscopy of lateral roots from the same promoter:GFP-GUS lines revealed that *UGT76B1* was mainly expressed in the root cortex and endodermis (Figure 8E). GUS staining of aerial plant parts showed *UGT76B1* expression in very young leaves (Figure 8B), hydathodes (Figures 8C and 8F), sepals, and style (Figure 8H). Expression in mature leaves of young plants (17 d) was patchy (Figure 8F). In 4-week-old plants, expression in leaves was reduced (Figure 8G). GUS staining also showed induction of *UGT76B1* expression after *P. syringae* inoculation and wounding (Figures 8I and 8J).

Nontargeted Metabolome Analysis Reveals Correlation between ILA Hexoside Formation and *UGT76B1* Expression

Since there was neither an indication of the UGT76B1 substrate nor of the affected metabolic pathway, we embarked on a completely nontargeted strategy to obtain this information. An ultra-high-resolution 12 Tesla FT-ICR mass spectrometer run in the negative ionization mode was employed to compare the metabolic profile of *UGT76B1-OE* and *ugt76b1* mutants with their respective wild type. Root material from plants grown in hydroponic culture was used as starting material for metabolite extraction because *UGT76B1* was mainly expressed in roots and showed only lower expression in leaves under unstressed conditions. A stringent, combinatorial screening for metabolite changes was performed across the two independent knockout lines in two different wild-type backgrounds and both independent overexpression lines. By setting a P value cutoff smaller than 0.01 and by filtering for metabolites that showed consistent and opposite regulation in knockout and overexpression plants, only two metabolites were found whose accumulation was significantly and positively correlated with *UGT76B1* expression. Both mass-to-charge ratio (*m/z*) peaks were repressed in the knockout and induced in the overexpression lines (Figure 9A; see Methods). In addition, both peaks were significantly enhanced compared with the wild type in leaf material of the *UGT76B1* overexpression lines, although with an overall lower intensity than in roots (see Supplemental Figure 6 online).

Due to the high accuracy in *m/z* determination, an exact molecular formula could be assigned to both peaks. Fragmentation studies further indicated that the molecule with *m/z* 293 was a glucoside (Figure 9B). No hexoside loss could be observed upon fragmentation of the second peak (*m/z* 279). Loss of the
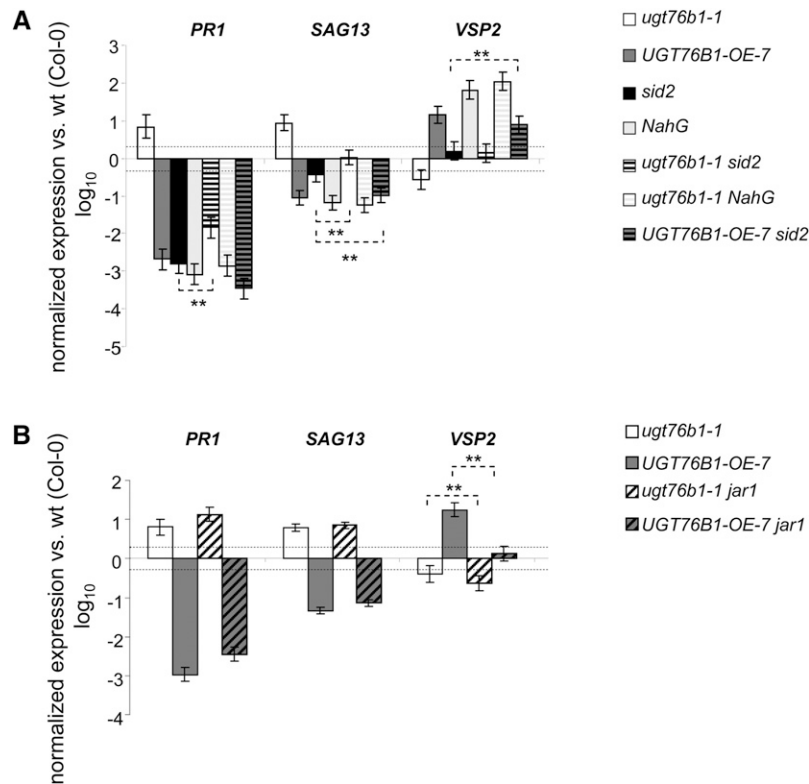
Figure 6. SA and JA Marker Gene Expression in *UGT76B1* Overexpression and Knockout Lines after Introgression into *sid2*, *NahG*, and *jar1*.

(A) Gene expression in *sid2* and *NahG* introgressed lines. Wt, wild type.
(B) Gene expression in *jar1* introgressed lines.
PR1, *SAG13*, and *VSP2* transcripts were quantified in 4-week-old *ugt76b1-1*, *UGT76B1-OE-7*, and the crossed lines by qRT-PCR. Expression levels were normalized to *UBIQUITIN5* and *S16* transcripts; levels relative to Col-0 plants are displayed. Arithmetic means and standard errors from log$_{10}$-transformed data of at least four independent replicates from two separate experiments were calculated using ANOVA. Asterisks indicate significance of the difference between the two bars indicated by the ends of the dotted line; **P value < 0.01.

hexosidic moiety from *m/z* 293 led to a smaller compound with *m/z* 131. The molecular formula of this residual aglycon was $C_6H_{12}O_3$. Further in-cell fragmentation of this molecule led to the loss of a formic acid (CH_2O_2) moiety and the formation of a second fragment, *m/z* 85. According to a previous study, this behavior indicated that the aglycon of *m/z* 293 was an α-hydroxy carboxylic acid with a free β-hydrogen (Bandu et al., 2006). Thus, six possible structures could be suggested for the aglycon *m/z* 131 (Figure 9C). Structures A, C, D, and F could be excluded because the fragmentation of the corresponding standard compounds gave rise to further fragments, which were not detected after fragmentation of the unknown aglycon from the plant extract (*m/z* 131) (see Supplemental Figure 7 online). Both compounds B and E gave the same fragmentation pattern as the unknown plant peak and therefore constituted possible candidate structures of the aglycon.

### In Vitro Activity of Recombinant UGT76B1 toward ILA

To further elucidate the structure of *m/z* 131, compounds B and E were tested as potential substrates of recombinant UGT76B1 in

vitro. UGT76B1 glucosylated ILA (compound B, 2-hydroxy-3-methylpentanoic acid), whereas it showed no activity toward 2-ethyl-2-hydroxybutyric acid (compound E) (Figures 10A to 10C; see Supplemental Figure 8 online). Thus, ILA turned out to be a substrate of UGT76B1 in vitro, which was in accordance with the observation of plant extracts derived from *ugt76b1* knockout and *UGT76B1-OE* lines. As we had found high levels of SA conjugates in the *UGT76B1* overexpression line, we also tested the activity of the recombinant protein toward SA. We could indeed observe the formation of SA Glc conjugate(s), although only a minor peak compared with the substrate SA was detected (Figures 10D to 10F).

The Direct Effect of ILA on Root Growth and Defense Mechanisms

The identification of ILA as a substrate of UGT76B1 raised the question of whether ILA itself was an active compound in planta. Indeed, exogenously applied ILA strongly affects plant root growth and defense marker gene expression. First, ILA inhibits root growth in a concentration-dependent manner (Figure 11A).
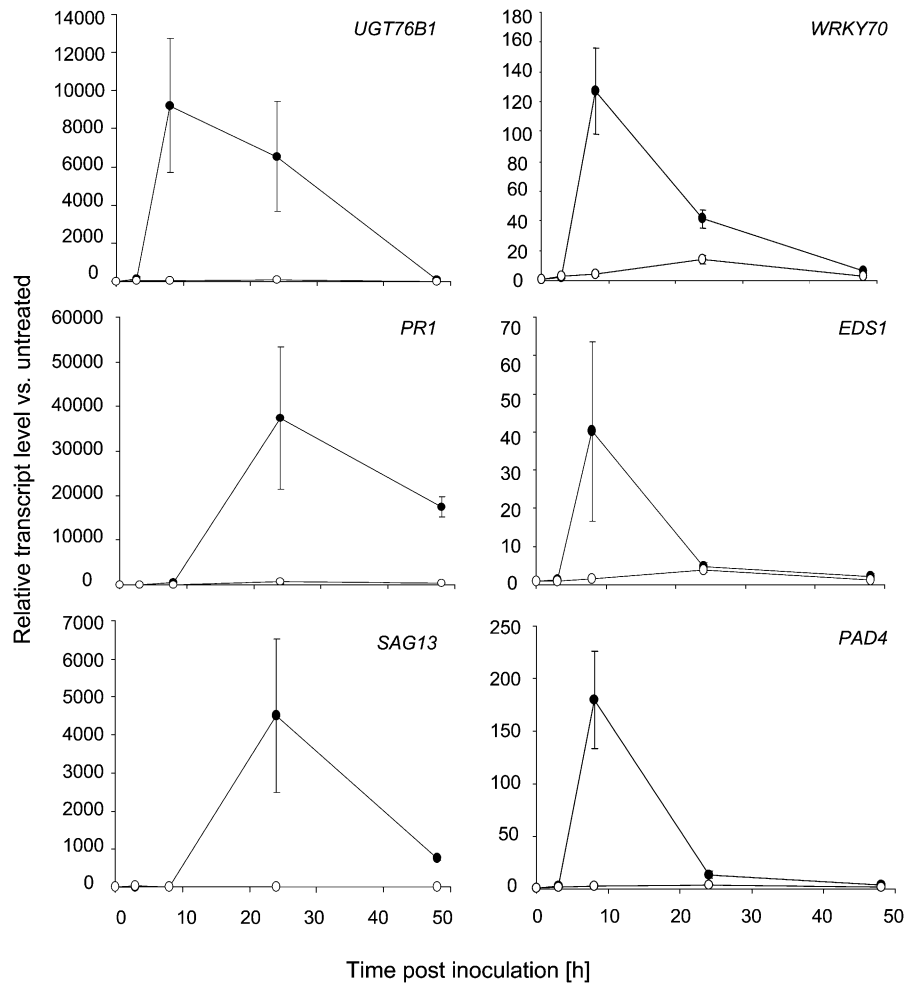
Figure 7. qRT-PCR Expression Profiles of *UGT76B1*, *WRKY70*, *EDS1*, and *PAD4* Induction after Infection with Avirulent *P. syringae.*

Transcript levels were quantified at the indicated time points after inoculation with *Ps-avir* (closed circles) and mock (10 mM MgCl$_2$; open circles) treatment. The transcript level (relative expression) was normalized to the transcript abundance of *UBIQUITIN5* and *S16* genes. Values correspond to the mean and standard deviation of triplicates. The experiment was repeated with similar results.

This repressive effect of ILA on root growth was more pronounced in *ugt76b1-1* than in the wild type, but on the other hand was ameliorated by the overexpression of *UGT76B1*, suggesting that the ILA aglycon was the active agent and glucosylation antagonized its effect. Furthermore, it was crucial to test whether ILA could affect plant defense pathways. Twenty-four hours after spraying an ILA solution onto leaves of 4-week-old plants, *PR1* expression was >10-fold induced, indicating a direct and positive influence on the SA pathway. By contrast, the JA marker genes *VSP2* and *PDF1.2* were not significantly influenced; while *VSP2* was only marginally suppressed, *PDF1.2* showed a tendency for induction but was highly variable as well (Figure 11B). In addition, ILA could also affect the strong *PR1* repression found in *UGT76B1-OE-7*, which was partially reverted (see Supplemental Figure 9 online). Since ILA induced the defense marker gene *PR1*, we were interested in determining whether this translated into an enhanced resistance toward *P. syringae*.

Indeed, plants that had been treated with ILA before infection by *Ps-avir* showed about four- to fivefold less bacterial growth compared with mock treatment (Figure 11C). The increased resistance was persistent for at least 1 to 3 d after ILA spraying. Optimization of the spraying regime and/or the use of surfactants might further enhance the protective effect.

DISCUSSION

Plant secondary metabolite glycosyltransferases constitute a large enzyme family. They are presumed to be involved in the biosynthesis, homeostasis, and regulation of the activity of numerous small molecule compounds in plants. However, enzyme-substrate relations and physiological roles of individual isoforms remain mostly obscure. To extend the knowledge of UGTs, we used publicly available databases to identify
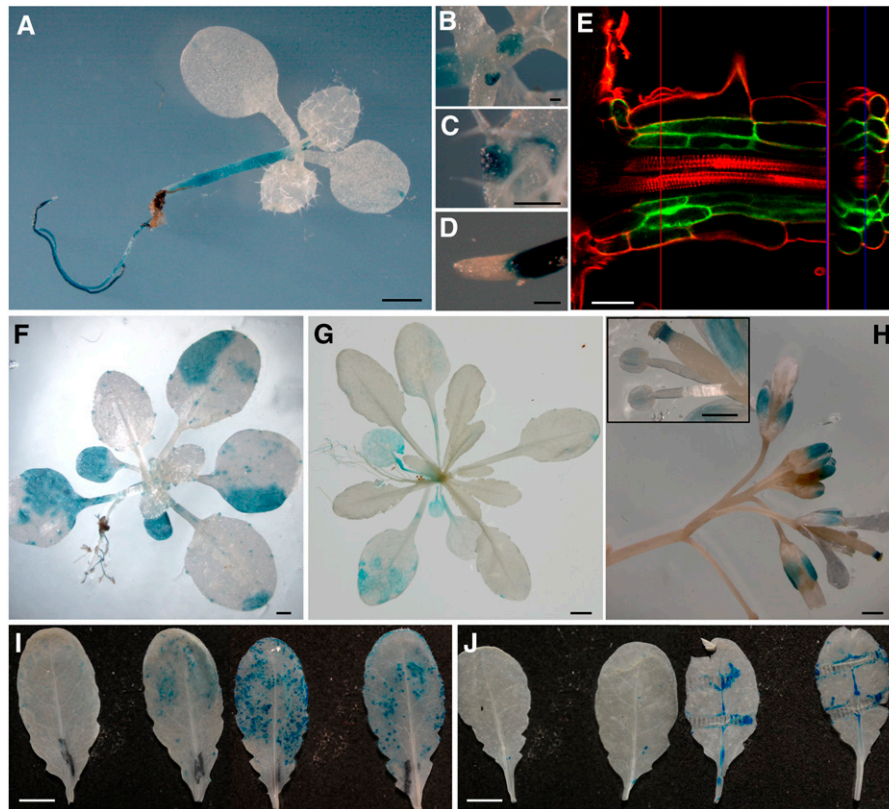
Figure 8. Localization of *UGT76B1* Expression Using *UGT76B1~pro~:GUS-GFP* Lines.

Transgenic plants harboring *UGT76B1~pro~:GUS-GFP* constructs were stained for GUS activity in different developmental stages (**[A]** to **[D]** and **[F]** to **[J]**) or examined for GFP fluorescence by confocal microscopy **(E)** (see Methods). Results were consistent among at least two independent transgenic lines.
(A) to **(D)** Eight-day-old seedling **(A)** with leaf primordia **(B)**, leaf hydatodes **(C)**, and root tip **(D)**.
(E) Lateral root of a 1-week-old seedling grown on an agar plate. Cell walls were counterstained with propidium iodide. The red and blue lines indicate the positions where the vertical (right part) and longitudinal (left part) optical cross sections were taken, respectively. Vertical and longitudinal projections are separated by the purple line.
(F) A 17-d-old plant.
(G) A 28-d-old plant.
(H) Inflorescence of a 36-d-old plant. The inset shows a magnification of the stigma and anthers.
(I) Two leaves of 5-week-old plants 8 h after mock treatment (left) or after inoculation with *Ps-avir* (right).
**(J)** Two leaves before (left) or 6 h after (right) mechanical wounding using a forceps.
Bars = 1 mm in **(A)** and **(F)**, 0.1 mm in **(B)** to **(D)**, 30 μm in **(E)**, 0.5 cm in **(G)**, **(I)**, and **(J)**, and 0.5 mm in **(H)**.

stress-induced *UGT* candidates, which might relate them to plant responses to biotic and abiotic stresses. *UGT76B1* was the top-ranking isoform among stress-responsive UGTs (Figure 1), and it is present as a single isoform in its subclass (Ross et al., 2001). Analysis of related *Brassicaceae* genomes revealed a highly conserved, single-copy homolog (M. Das and G. Haberer, personal communication). These features suggested a unique and important function of *UGT76B1* in plant stress responses.

Nontargeted Metabolomics Approach Leads to Identification of UGT76B1 Substrate

Despite major advances in plant biology due to genome annotations and omics approaches, a majority of gene products are still orphan enzymes without specific substrates and physiolog-

ical roles (Fridman and Pichersky, 2005; Saito et al., 2008; Hanson et al., 2010). Although the annotation of an enzyme, for instance as a UGT, most probably denotes its activity as a transferase of an activated sugar onto small-molecule acceptors, this knowledge does not provide a clue toward its native substrate(s) or of its in vivo function. In the case of UGTs, even sequence homology to already known isoforms does not allow to deduce substrate classes (Vogt and Jones, 2000; Bowles et al., 2006). Nevertheless, integration of metabolite profiling with independent evidence, in particular of transcriptional coexpression and comparative genomics, has strongly assisted the elucidation of metabolic pathways and assignment of enzymatic activities (Hirai et al., 2005; Yonekura-Sakakibara et al., 2008; Matsuda et al., 2009; Ohta et al., 2010). In the case of the broadly stress-inducible *UGT76B1* gene, coexpression analyses did not
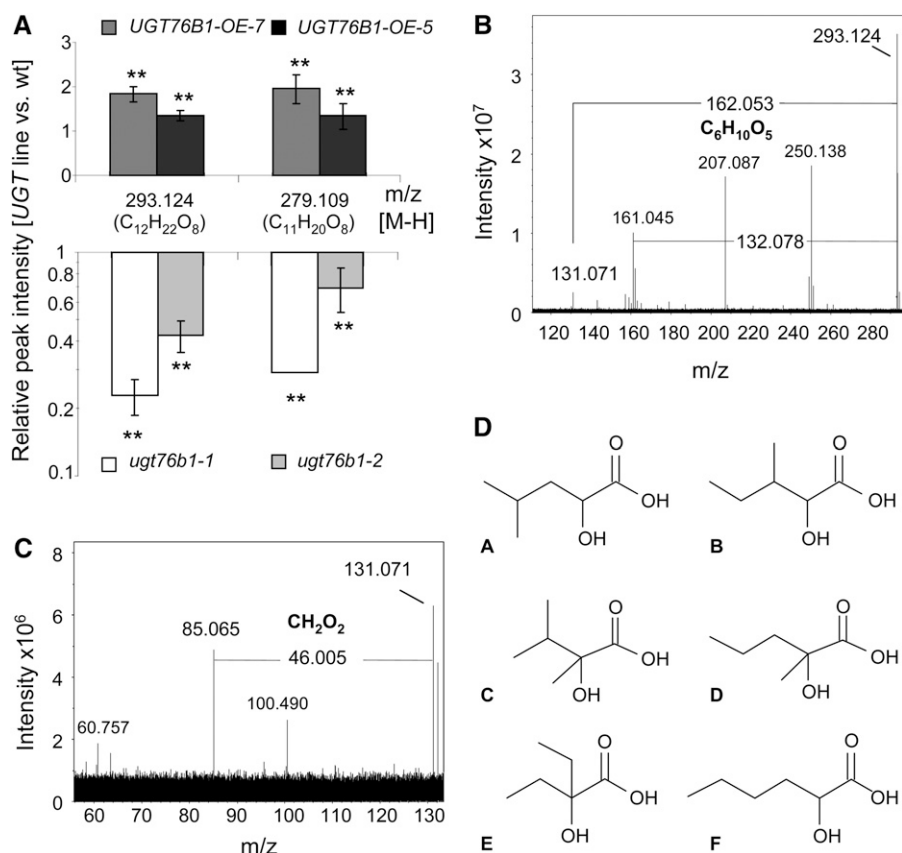
Figure 9. Nontargeted Metabolome Analysis of *UGT76B1* Overexpression and *ugt76b1* Knockout Lines.

(A) Metabolic changes found in roots of two independent knockout lines and two independent overexpression lines compared with the respective wild type (wt). Means and standard deviation of three independent biological replicates with two technical replicates each are displayed. *m/z* 279 was nearly undetectable and undetectable in *ugt76b1-2* and *ugt76b1-1*, respectively. Therefore, a default value for the *ugt76b1-1* peak was used for calculating the relative intensity (see Methods). Asterisks indicate significance of the difference to the wild type; **P value < 0.01. The predicted molecular formulae are indicated. The experiment was independently repeated with similar results.

(B) Fragmentation pattern of *m/z* 293. The loss of *m/z* 162 confirmed the presence of a hexosidic moiety. Other major peaks at *m/z* 207 and 250 could be unequivocally excluded as *m/z* 293–derived fragments; they were originating from electrical noise and from an N-containing contaminant, respectively. By contrast, *m/z* 161 was in agreement with a radical anion of deprotonated hexose, which was directly produced from *m/z* 293.

(C) Further in-cell fragmentation led to the elimination of CH_2O_2 (formic acid), which restricted the nature of the aglycon to α-hydroxy carboxylic acid isomers.

**(D)** Six possible isomeric molecular structures of the aglycon $C_6H_{12}O_3$.

indicate an association with particular pathways, which could hint toward a class of potential substrates. Thus, we aimed to use a nontargeted approach employing ultra-high-resolution FT-ICR MS to obtain information on the affected pathway or substrate without any other prior knowledge. Nontargeted FT-ICR MS data are well suited to identify and differentiate metabolic patterns from distinct situations based on multivariate analyses (Ohta et al., 2010). In contrast with this approach, we did a pairwise comparison of *m/z* values from crude extracts of *UGT76B1* overexpression, *ugt76b1* loss of function, and wild-type lines. Only two peaks fulfilled the criteria of being both underrepresented in two independent knockout lines (in different accessions as background) and upregulated in two independent overexpression lines (Figure 9A). Thus, this combinatorial approach allowed us to pinpoint informative molecules from the

nontargeted metabolome analyses. Since further fragmentation of these *m/z* peaks indicated that one of them was a hexoside, it was highly suggestive that it indicated the in planta product of UGT76B1. Eventually, enzymatic tests using the recombinant enzyme proved its ability to glucosylate the predicted aglycon in vitro and thereby established ILA as a substrate of UGT76B1.

UGT76B1 Affects SA-JA Crosstalk and Is Affected by the SA and JA Pathways

SA and JA defense signaling pathways are known to interact in a mostly antagonistic manner (Kloek et al., 2001; Spoel et al., 2003; Koornneef and Pieterse, 2008). Both *UGT76B1* overexpression and loss of function led to a disturbed equilibrium between these two pathways, suggesting a role for *UGT76B1* in
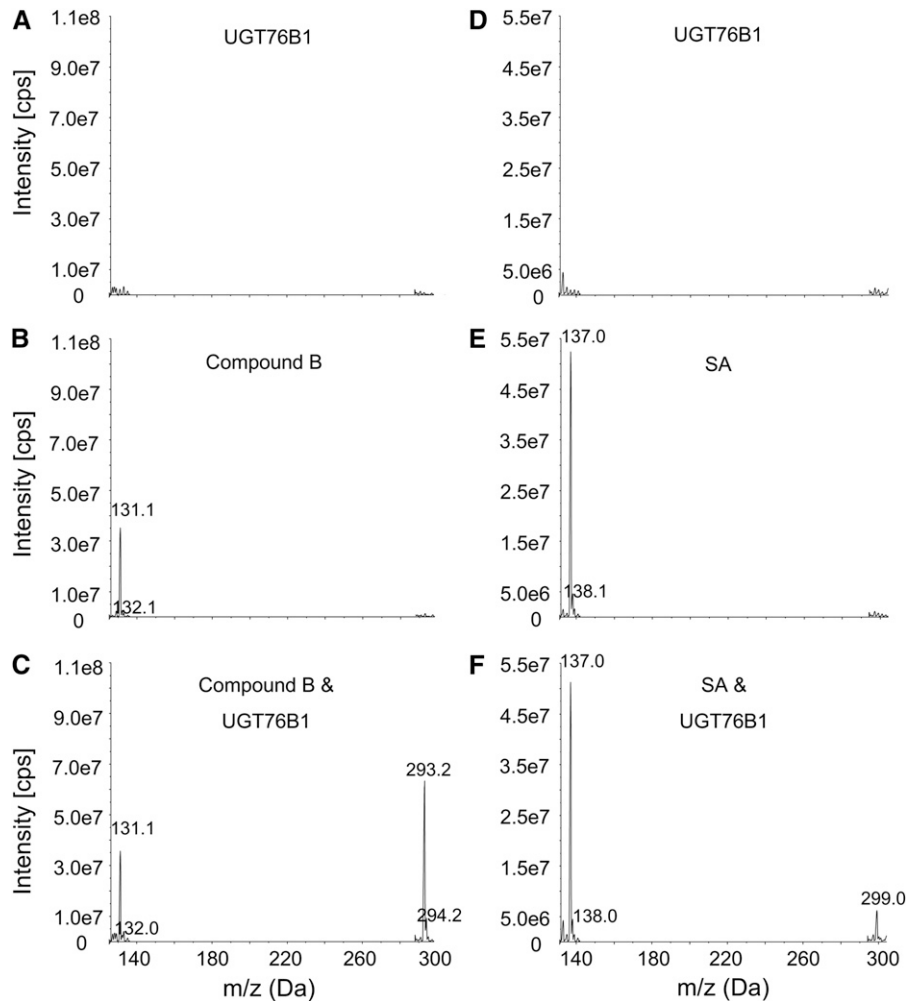
Figure 10. In Vitro Activity Assay of UGT76B1.

Activity of recombinant UGT76B1 was tested with ILA (2-hydroxy-3-methylpentanoic acid, compound B) (**[A]** to **[C]**) and SA (**[D]** to **[F]**). The reactions were analyzed by mass spectrometry (see Methods). The *m/z* values of the corresponding substrates and products are indicated. The experiment was independently repeated with similar results.
(A) and **(D)** Mass spectra of enzyme reactions without substrate.
**(B)** and **(E)** Mass spectra of enzyme reactions without enzyme.
(C) and **(F)** Mass spectra of complete reactions.

SA-JA crosstalk. The complete loss of *UGT76B1* function led to constitutive enhancement of the SA-dependent defense and repression of the JA pathway, whereas *UGT76B1* overexpression led to the opposite effects (Figures 4 and 12). Accordingly, knockout plants were more resistant to infection by a biotrophic pathogen but more susceptible to necrotrophic attack, while the opposite was true for the overexpression line (Figure 3). Knowing that *UGT76B1* suppresses the SA-dependent pathway, it seems surprising at first glance that its expression was induced after *P. syringae* infection within the same time frame as the SA-dependent marker genes *PAD4*, *EDS1*, and *WRKY70* and prior to *SAG13* and *PR1* (Figure 7). This finding indicates that *UGT76B1* might play a role in suppressing the SA response in unchallenged conditions, while being required to attenuate it

after pathogen attack. Controlled suppression of defense responses is important to avoid deleterious consequences and significant costs for the plant (see Introduction).

UGT76B1 was shown to be induced by both SA and methyl jasmonate in microarray expression studies (Zimmermann et al., 2005). Consistent with these findings and its role in promoting the JA pathway, *UGT76B1* was induced after wounding (Figure 8J). The constitutive expression of *UGT76B1* in hydathodes and young tissues (Figures 8B and 8C) could be involved in the local enhancement of the JA pathway, providing protection against herbivores or necrotrophs at these more vulnerable sites (Hugouvieux et al., 1998; Sprague et al., 2007).

The induction or repression of *UGT76B1* in several mutants, in which the SA pathway is affected in unstressed conditions,
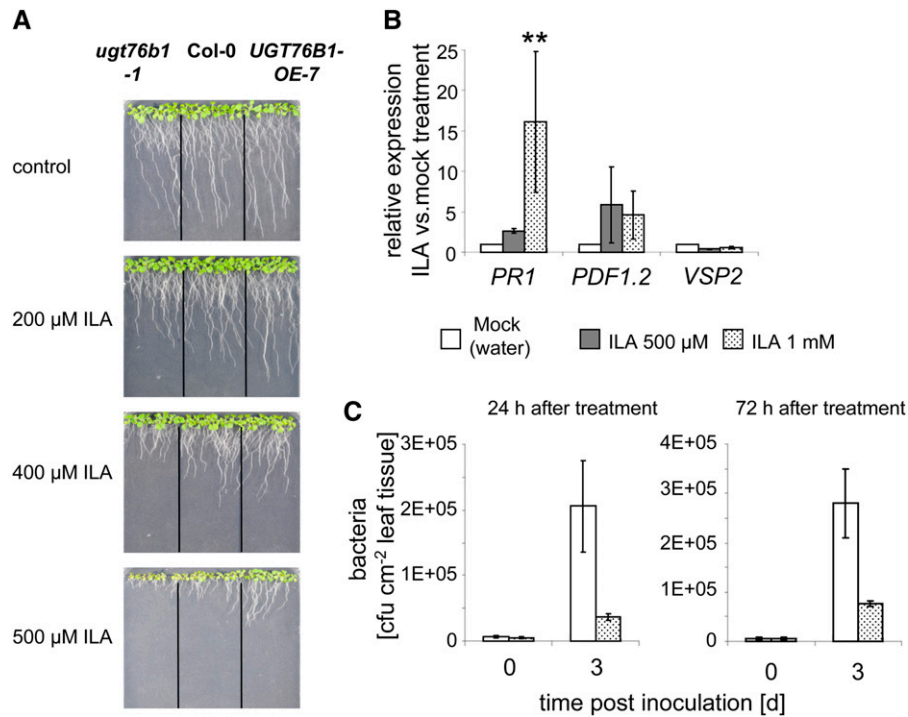
Figure 11. The Direct Effect of Exogenously Applied ILA.

(A) Root growth inhibition phenotype of ILA inversely correlates with *UGT76B1* expression. Photographs were taken 10 d after sowing the seeds on plates containing 0, 200, 400, and 500 µM ILA.

(B) Defense marker gene expression in Col-0 plants after ILA treatment. Transcript levels of *PR1*, *PDF1.2*, and *VSP2* in leaves of 4-week-old Col-0 plants 24 h after ILA or water treatment were quantified by qRT-PCR. Values are relative to the expression 24 h after mock (water) treatment. Graph represents the mean and SD of three biological replicates. **P value < 0.01.

(C) Bacterial growth in *Arabidopsis* leaves of wild-type plants sprayed with water (white) or 1 mM ILA (dotted) before infection. Plants were inoculated with 5×10^5 cfu mL^{-1} of *Ps-avir* 24 or 72 h after treatment, and bacteria (cfu cm^{-2}) were quantified 0 and 3 d after inoculation. The graphs represent the means and SD of three replicates.

[See online article for color version of this figure.]

provided additional evidence that the glucosyltransferase is correlated with this defense pathway (see Supplemental Figure 10 online). Profiling of *UGT76B1* expression in *Arabidopsis* mutants *cpr5*, *mkk1 mkk2*, and *mpk4* revealed that the gene was highly induced in these plants, which display constitutively enhanced SA-dependent defenses (Bowling et al., 1997; Brodersen et al., 2006; Pitzschke et al., 2009). By contrast, *UGT76B1* expression was suppressed in mutants such as *eds1*, *sid2* (*eds16*), and *pad4* (Glazebrook et al., 1996; Feys et al., 2001; Wildermuth et al., 2001), which are impaired in SA-dependent responses (Zimmermann et al., 2005). Many SA-dependent gene regulations are mediated by NPR1 (Vlot et al., 2009). However, the induction of UGT76B1 can at least partially occur in an NPR1-independent manner, since SA could enhance its expression also in the *npr1-1* mutant (Blanco et al., 2009). In addition, *npr1-1* versus wild type expression analyses indicated an activation of *UGT76B1* in the *npr1* loss-of-function mutant (see Supplemental Figure 10 online).

There is a considerable overlap between genes involved in defense and senescence signaling. In particular, enhanced SA levels promote senescence-related processes, and some genes involved in the senescence process seem to be directly regulated by SA (Quirino et al., 1999; Morris et al., 2000; Miao and Zentgraf, 2007). Consistently, several of the mutants discussed above that display constitutive expression of SA-related defense responses frequently show an accelerated onset of senescence as well (Yoshida et al., 2002; Barth et al., 2004; Consonni et al., 2006), whereas an SA-deficient *NahG* line showed delayed developmental senescence (Buchanan-Wollaston et al., 2005). Conversely, plant stress responses are also known to be affected by leaf age (Kus et al., 2002), a phenomenon described as age-related resistance. In the case of *ugt76b1*, we could exclude age-related resistance (see Supplemental Figure 4 online) and, therefore, further analyzed the link between constitutive induction of SA-dependent defense and the onset of senescence. Both induction of the senescence marker gene *SAG13* and early leaf yellowing in *ugt76b1-1* were shown to be dependent on SA levels in these plants, since crossing into the *sid2* or *NahG* background reverted these phenotypes (Figure 6; see Supplemental Figure 5 online). On the other hand, *PR1* and *SAG13* transcript levels in the *UGT76B1* overexpression line are comparable to those found in *NahG* (Figure 6).
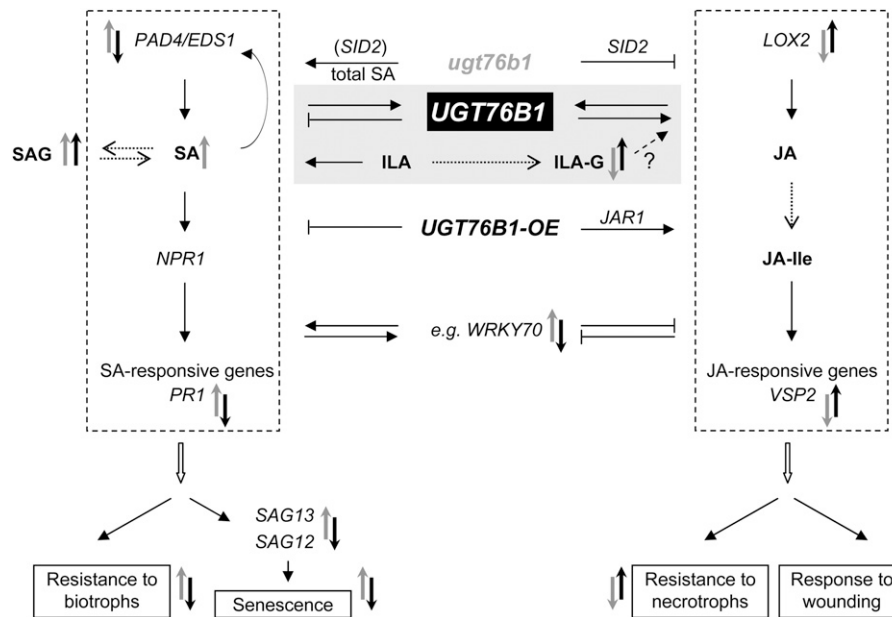
Figure 12. Model of the Involvement of UGT76B1 as a Novel Mediator in SA- and JA-Dependent Regulation of Defense Responses and Senescence.

The model relates UGT76B1 to SA and JA pathways regulating defense against (hemi-) biotrophic and necrotrophic pathogens. Key steps of both pathways are shown. *UGT76B1* induces the JA response and represses the SA-dependent pathway, stimulating defense against necrotrophs and having a negative influence on the resistance to *P. syringae* and the onset of senescence. The UGT76B1 substrate ILA enhances the SA pathway. The consequences of gain and loss of *UGT76B1* function are integrated along with their dependence on *SID2* and *JAR1*. Signaling molecules (SA, SAG, JA, JA-Ile), enzymatic transformations (dashed and open arrows), activation (closed arrows), suppression (line with vertical bar), and important genes are indicated. Positive and negative influences of *ugt76b1* (gray) and *UGT76B1-OE* (black) are shown, respectively.

Collectively, these data suggest that *UGT76B1* is a novel player in the SA-JA crosstalk, acting as a negative modulator and attenuator of the SA response, while it positively affects the JA-dependent pathway (Figure 12). However, the general stress perception and SA/JA signal transduction pathways were preserved and independent of *UGT76B1* expression. This was demonstrated by the full inducibility of *PR1* after pathogen infection in *UGT76B1-OE-7* and by the root growth inhibition upon methyl jasmonate treatment in *ugt76b1-1* (Figure 4B; see Supplemental Figure 11 online).

Integration of *UGT76B1* in SA-JA Crosstalk

To further examine the integral role of *UGT76B1* in SA-JA crosstalk, *UGT76B1* knockout and overexpression lines were crossed into mutants compromised in either the SA or JA response. These genetic analyses indicated that both the induction of the SA pathway and the repression of JA responses in *ugt76b1* were dependent on SA (Figures 6 and 12). Thus, inhibition of JA-dependent defense in *ugt76b1* seemed to be mediated by the known antagonism caused by the enhanced SA level and SA-related signaling in this line. The transcription factor WRKY70 is an important player integrating signals from the antagonistic JA and SA pathways, suggested to be located downstream of NPR1. It acts as a negative regulator of JA-responsive genes and as a positive regulator of SA-induced genes and resistance to *P. syringae* and might act downstream of the biosynthesis of both

hormones (Li et al., 2004; Glazebrook, 2005; Ülker et al., 2007). In this work, enhanced WRKY70 expression in the *ugt76B1* knockout was positively correlated with SA signaling but also SA biosynthesis. Therefore, UGT76B1 might overrule the effects of WRKY70 and the latter may only be involved in the SA-mediated suppression of the JA pathway (Figure 12).

Although the pathogen phenotypes and marker gene analyses showed a clearly opposite pattern in *ugt76b1* knockout and *UGT76B1* overexpression lines, their link to the SA and JA pathways was not simply inverse. In contrast with the SA-mediated *ugt76b1* knockout phenotypes, the enhancement of the JA pathway in the *UGT76B1* overexpression line was *JAR1* dependent and did not rely on the suppression of *SID2*. Since basal levels of free SA were not significantly repressed in *UGT76B1-OE*, it is not clear whether the *JAR1*-dependent enhancement of the JA pathway is related to a suppressive action on the SA pathway (Spoel et al., 2003). Another possibility would be that UGT76B1 directly influences the JA pathway. Such an UGT76B1-dependent stimulation of the JA pathway in the overexpression line could be regulated via enhanced ILA glucoside levels or another UGT76B1-related function, yet both mechanisms would require *JAR1* (Figure 12).

The dependence of several aspects of UGT76B1 action on SA and the side activity of the recombinant enzyme toward SA also prompted us to consider UGT76B1 as a SA-conjugating enzyme. Two SA-glucosylating enzymes were described in *Arabidopsis*. Both UGT74F1 and UGT74F2 were shown to

greatly contribute to the formation of SAG and SA Glc ester in vivo, respectively, but the possibility could not be excluded that additional enzymes were involved in SAG biosynthesis (Dean and Delaney, 2008). However, the enhanced levels of free SA and SA glucosides in the *ugt76b1* knockout (Figure 5) did not support a role for UGT76B1 as an SA glucosyltransferase, unless the loss of an SA glucosyltransferase would increase free SA and activate other enzymes and therefore lead to even higher glucosylating activity than in the wild type. This scenario, however, is not likely to occur, since neither *ugt74f1* nor *ugt74f2* single mutants resulted in enhanced glucosylation of exogenously applied SA (Dean and Delaney, 2008). Instead, the enhanced levels of both SA and SAG in *ugt76b1* are reminiscent of conditions in other mutants showing constitutive activation of SA-dependent defense, such as *cpr20* (Silva et al., 1999), *cpr5* (Bowling et al., 1997), and *cpr30* (Gou et al., 2009), and of the plant's normal response to a biotrophic pathogen stimulus.

By contrast, the contribution of the SA-conjugating activity to the *UGT76B1* overexpression phenotype cannot be fully excluded. However, the *UGT76B1-OE* line exhibited the same level of *PR1* induction upon *P. syringae* infection as the wild type (Figure 4B). This is in contrast with the finding for the established SA glucosyltransferase UGT74F2; *UGT74F2-OE* lines were considerably impaired in their ability to induce *PR1* after *P. syringae* infection, which is in line with UGT74F2's ability to glucosylate SA and thereby suppress SA-dependent defense (Song et al., 2008).

Our combined data on UGT76B1's enzymatic activity toward ILA, the correlation of ILA glucoside levels with *UGT76B1* expression in vivo, the altered pathogen susceptibility of the *ugt76b1* knockout line, as well as the direct effect of exogenous ILA on defense marker gene expression and *P. syringae* resistance suggest that the endogenous role of UGT76B1 and its relation to the SA and JA pathway is primarily related to its activity on ILA.

Amino Acid–Related ILA and Plant Defense

The direct link between the activity of UGT76B1 toward ILA and SA-dependent defense was established by the finding that exogenously applied ILA enhanced resistance toward *PS-avir* (Figure 11). *PR1* expression was induced to a level similar to the induction found in *ugt76b1*. Accordingly, the lack of ILA glucosylation in the knockout line could lead to the induction of SA-dependent signaling. On the other hand, *UGT76B1* overexpression leads to increased glucosylation of ILA and, therefore, reduced *PR1* expression. In line with this, ILA application could partially revert the strong *PR1* repression in *UGT76B1-OE*. These data suggest that the ILA aglycon and not the glucoside is active in enhancing the SA pathway and *PR1* expression. ILA was also likely the biologically active compound in another bioassay. Exogenous ILA inhibited root growth, and this effect was more pronounced for *ugt76b1* but ameliorated in the *UGT76B1-OE* line. How ILA is perceived at the molecular level and at which step it activates the SA or other pathways is currently not clear and requires further investigation (see also below). Interestingly, ILA did not significantly reduce the expression of JA marker genes *VSP2* and *PDF1.2*; the latter even showed a tendency for upregulation. Thus, exogenous ILA did not affect the SA and JA pathways in an antagonistic manner, which suggests that it may have biotechnological applications as a plant protective agent. In fact, SA and JA are not exclusively antagonistic, and even synergistic action has been reported for SA and JA dependent on their concentration and timing (Mur et al., 2006). Accordingly, exogenous ILA could interfere with the SA and JA pathways at this level.

Neither ILA itself nor its glucoside had been described before in plants. However, ILA has been characterized in humans as the reduced form of 2-keto-3-methylvaleric acid, a degradation product of the branched-chain amino acid Ile (Mamer and Reimer, 1992; Podebrad et al., 1997). A genetic defect in the further oxidation of this product led to its accumulation along with other degradation products and the amino acids themselves in maple syrup urine disease (Mamer and Reimer, 1992).

A correlation analysis based on microarray data at ATTED-II and VirtualPlant (Obayashi et al., 2009; Katari et al., 2010) provided evidence for a relationship between ILA and amino acid metabolism also in *Arabidopsis*. *UGT76B1* expression correlated with that of *LIPOAMIDE DEHYDROGENASE2* (see Supplemental Figure 12 online), a gene encoding a component of the branched-chain keto acid dehydrogenase complex, which catalyzes the oxidative decarboxylation of the α-keto acid derivatives of Val, Leu, or Ile (Binder et al., 2007). The second compound with *m/z* 279 ($C_{11}H_{20}O_8$) found to be correlated with *UGT76B1* expression in our nontargeted metabolomics approach differed from the ILA-glucoside peak (*m/z* 293, $C_{12}H_{22}O_8$) by one CH_2 moiety. This could represent the corresponding glucosylated compound derived from Val metabolism (2-hydroxy-3-methylbutyric acid [valic acid]). Therefore, we evaluated the biological activity of this putative analog of ILA. Indeed, valic acid showed a similar but weaker inhibition of root growth compared with ILA, and recombinant UGT76B1 was able to glucosylate valic acid (see Supplemental Figure 13 online).

Amino acid–derived molecules have also been related to *Arabidopsis* defense reactions by the involvement of two aminotransferases, ALD1 and AGD2, which supposedly catalyze an amino transfer in opposite directions while acting on an unknown α-keto acid/α-amino acid couple (Song et al., 2004). These authors found that *agd2* mutants were more resistant to *P. syringae* infection, while *ald1* showed increased susceptibility. Furthermore, plant hormones are known to be regulated by conjugation with amino acids. In particular, Ile is known to be conjugated to JA to form JA-Ile, the main bioactive form of the hormone (Staswick and Tiryaki, 2004; Fonseca et al., 2009). SA can be also conjugated to amino acids (reviewed in Vlot et al., 2009), and overexpression of GH3.5, an enzyme potentially involved in this conjugation, led to enhanced pathogen resistance and SA accumulation (Park et al., 2007).

Due to the close relationship between ILA and the amino acid Ile, one may also speculate that ILA or its glucoside has an impact on amino acid–related hormone conjugations via a yet unknown mechanism. Thus, future research should focus on the relationship between plant defense pathways, amino acid–derived metabolites, and small-molecule glucosylation.

METHODS

Plant Materials and Growth Conditions

Two T-DNA insertion lines in two different wild-type backgrounds, *ugt76b1-1* (SAIL_1171A11 [Col-0]) and *ugt76b1-2* (GT_5_11976 [L*er*]), were obtained from the Nottingham Arabidopsis Stock Centre (Scholl et al., 2000). The published position of the T-DNA insertion was confirmed by PCR and DNA sequencing using the primers 5′-TTCATAAC-CAATCTCGATACAC-3′ and 5′-GTCTGATTATGGGAATGCAGATTA-3′ (76B1_R) for the SAIL (Syngenta Arabidopsis Insertion Library) line and primers 5′-CGTTTTGTATATCCCGTTTCCGT-3′ and 5′-AAGATCCAAGAT-CAGGGGATAAG-3′ (76B1_F) for the GT-5 line, respectively. A 3:1 segregation of the respective resistance (BASTA for SAIL and kanamycin for GT-5) after backcrossing indicated that the mutation was inherited as a single locus in both cases. RT-PCR analysis using the gene-specific primers 76B1_F and 76B1_R confirmed the lack of *UGT76B1* transcripts in both lines (see Supplemental Figure 1 online).

UGT76B1 overexpression lines were produced by *Agrobacterium tumefaciens*–mediated transformation using plasmids carrying the open reading frame coupled to cauliflower mosaic virus 35S-derived promoters in two different vectors, pB2GW7 and pAlligator2 (Clough and Bent, 1998; Karimi et al., 2002; Bensmihen et al., 2004). The following primers were used for *UGT76B1* amplification and cloning using GATEWAY (Invitrogen) recombination: 5′-GGGGACAAGTTTGTACAAAAAAGCAGGCTACACAAT-GGAGACTAGAGAAACAAAACCA-3′ and 5′-GGGGACCACTTTGTACAA-GAAAGCTGGGTCTGATTATGGGAATGCAGATTA-3′. After selection of transformants, segregation analysis was used to identify single insertion lines in the T2 generation.

The point mutation lines *sid2-1* (Nawrath and Métraux, 1999) and *jar1-1* (Berger, 2002) were both crossed with *UGT76B1* loss-of-function and overexpression lines. The *NahG* transgenic line (Gaffney et al., 1993) was crossed with *ugt76b1-1*. The homozygosity of the resulting lines was confirmed by its JA-resistant root growth phenotype in the case of *jar1*. Homozygosity of *sid2-1* was confirmed by a cleaved amplified polymorphic sequence marker (Konieczny and Ausubel, 1993). PCR fragments were amplified using primers SID2_f, 5′-TGCTTGGCT-AGCACAGTTACA-3′, and SID2_r, 5′-AGCTGATCTGATCCCGACT-3′, and digested with *Mfe*I, which discriminated against a single C-to-T nucleotide substitution in *sid2-1*.

For infection experiments, qRT-PCR analysis, and plant transformation, plants were grown on soil (Floraton 1 or Floragard B fein; Floragard) under a 12- to 14-h light cycle at 45 μmol m^{-2} s^{-1} of light intensity at 18°C in the dark and 20°C in the light. For metabolic analysis of root material, plants were grown hydroponically at 120 μmol m^{-2} s^{-1} of light intensity. Seeds were surface sterilized and grown on plates with half-strength Murashige and Skoog medium (M5519; Sigma-Aldrich), 1% Suc, and 0.25% Gelrite. Seedlings were transplanted after 7 d in a floating hydroponic system (Battke et al., 2003) and grown for two more weeks. Each Vitro Vent box contained 300 mL liquid medium and 250 mL polypropylene granulate as the floating material.

Chemicals

Compounds A, E, F, and valic acid [(*S*)-(+)-2-hydroxy-3-methylbutyric acid] were obtained from Sigma-Aldrich and compound B [(2*S*, 3*S*)-2-hydroxy-3-methylpentanoic acid] from Interchim. Compounds C and D were not commercially available. Therefore, they were synthesized according to previously described protocols (Yabuuchi and Kusumi, 1999; Caille et al., 2009).

Dark-Induced Senescence

Excised leaves from 5-week-old plants grown under short-day photoperiodic conditions were kept for 5 d in the dark at room temperature (Oh et al., 1996).

Data Mining of Public Expression Data

A complete collection of 122 *UGT* genes from *Arabidopsis thaliana* was extracted via the CAZY database (www.cazy.org). No Arabidopsis Genome Initiative locus was associated with the two pseudogenes listed (*UGT85A6P* and *UGT90A3P*), and *UGT89B1* (At1g73880) was not represented on the ATH1 array. Among the residual 119 probe sets, 105 targeted individual members specifically, whereas seven did not discriminate between two highly homologous isoforms each. Normalized microarray data for all 119 probe sets comprising abiotic and biotic (without elicitors) stressors applied to Col wild-type seedlings were downloaded from the BAR database.

For a number of treatments, two or more time points had been deposited. In cases where both up- and downregulations were recorded, the difference between the total number of significant inductions (>1.5-fold) and repressions (<0.67) was calculated. A specific gene was assigned as "induced" when inductions were present in at least two time points and the number of inductions exceeded repressions in at least two consecutive time points. In cases where the number of inductions equaled repressions, genes were nevertheless assigned as induced if clear induction kinetics had been observed. In cases with only two experimental time points, induction in one instance was sufficient as long as no repression had been observed in the second time point. For final classification, the maximal induction among different time points was selected for each treatment. The total number of significant stress inductions was separately indicated for abiotic and biotic stress cues, and a mutual rank M_R [M_R = (rank abiotic $\times$ rank biotic)$^{0.5}$] (Obayashi et al., 2009)] for both biotic and abiotic stress inductions was calculated for each *UGT* isoform to sort genes from highest to lowest combined stress inducibility.

Real-Time qRT-PCR

Rosette leaves of the indicated age were collected. Total RNA was isolated using the RNeasy plant mini kit (Qiagen). RNA integrity and amount were analyzed by gel electrophoresis and spectrophotometry. One microgram of total RNA was reverse transcribed using a SuperScript II RT-PCR Kit (Invitrogen) according to the manufacturer's instructions.

Gene-specific primer pairs were designed using the Primer Express 3.0 software. Primer pairs are listed in Supplemental Table 1 online. All primer pairs were evaluated for amplification specificity and an efficiency of over 80% using a serial cDNA dilution. Real-time quantification was performed using a 7500 real-time PCR system (Applied Biosystems). Individual PCR reaction mixtures contained 4 μL of diluted cDNA, 10 μL of Sybr Green Mastermix (Thermo Scientific), and 250 μM of each primer in a final volume of 20 μL. In all experiments, three biological replicates of each sample and two technical (PCR) replicates were performed. The amount of target gene was normalized over the abundance of the constitutive *UBQ5* and *S16* genes. The stability of the reference genes was tested, and normalization was performed using GeNorm (Vandesompele et al., 2002). For qRT-PCR of infected material, plants were infected as described below. Three biological replicates were analyzed, each consisting of six individually infected leaves. Plant material was harvested before infection and mock treatments (time point 0) and at the indicated time points after treatment. Each experiment was repeated with similar results.

For marker gene analysis on uninfected material and senescent leaves, methods for paired or grouped data were applied, namely the paired *t* test

and repeated-measurement analysis of variance (ANOVA; linear mixed-effect models), in order to control for interplate variation (each replicate was measured on a different qPCR plate). Two-way ANOVA was used to join results from two independent analyses. First, a model with interaction was fitted. If the interaction effect was significant, one-way ANOVAs were performed for the single experiments; otherwise a two-way ANOVA without an interaction effect was fitted. All analyses (P value, arithmetic mean) were performed on log_{10}-transformed data as recommended in the literature (Rieu and Powers, 2009). For all calculations, R software with the nlme package was used (Pinheiro et al., 2009; R Development Core Team, 2009).

Pathogen Infections

Bacterial strains used in this study include *Pseudomonas syringae* pv *tomato* DC3000 (*Ps-vir*) and *P. syringae* pv *tomato* DC3000 (avrRpm1) (*Ps-avir*). Bacteria were grown overnight at 28°C in King's B medium with appropriate antibiotics (100 μg/mL rifampicin for *Ps-avir* and *Ps-vir* and 50 μg/mL kanamycin for *Ps-avir*) and diluted to 5×10^5 cfu mL^{-1} with 10 mM $MgCl_2$ for plant inoculation. Whole leaves of 5- to 6-week-old plants were infiltrated using a 1-mL syringe without a needle. Control plants were infiltrated with 10 mM $MgCl_2$. Leaf discs from control-treated and infected plants were harvested from inoculated leaves at 0, 1, and 3 d after infiltration. Bacterial growth was assessed as described previously (Katagiri et al., 2002). For each time point, three samples were made by pooling six leaf discs from three different treated plants.

Alternaria brassicicola strain CBS 125088 (Pogány et al., 2009) spores were used for fungal infections. Conidial suspensions (1.5×10^6 conidia mL^{-1} of distilled water) for the inoculation were prepared from 10- to 15-d-old *A. brassicicola* cultures grown on malt extract agar medium (15 g of malt extract and 7.5 g of agar per L; Merck) at 22°C with a 12-h-light/12-h-dark cycle. A 5-μL droplet of the spore suspension was transferred onto the adaxial surface of leaves (sixth to eleventh leaf). Plants were kept in the container covered with plexiglass before and after inoculation to maintain a high ambient humidity. Distilled water was used for mock treatment. Lesions on the inoculated leaves were recorded 10 to 13 d after inoculation.

Histochemical Localization of Gene Expression

A fragment upstream of the *UGT76B1* start codon was amplified from genomic DNA (accession Col-0) by PCR using primers 5′-GGGGA-CAAGTTTGTACAAAAAAGCAGGCTCGGTTAAACATAAACCATGT-3′ and 5′-GGGGACCACTTTGTACAAGAAAGCTGGGTGTCTCCATTTTTGTTGT-GAAT-3′ and introduced into vector pBGWFS7 (Karimi et al., 2002). The resulting *UGT76B1*$_{pro}$:*GUS-GFP* fusion construct was transformed into Col-0 *Arabidopsis* plants (Clough and Bent, 1998). After selection of transformants, segregation analysis was used to identify lines with single insertions in the T2 generation. Thus, two independent lines, *UGT76B1*$_{pro}$:*GUS-GFP-2* and *UGT76B1*$_{pro}$:*GUS-GFP-12*, were selected for further analysis.

Histochemical analysis of the GUS reporter gene was performed at different developmental stages according to Lagarde et al. (1996) using 1 mM each of potassium ferro- and ferricyanide. Ethanol (70%) was used for destaining chlorophyll. To gain more detailed information about *UGT76B1* expression in roots, the same *UGT76B1*$_{pro}$:*GUS-GFP* lines were analyzed with a confocal laser scanning microscope (LSM 510 Axiovert 100M; Carl Zeiss). For cell wall staining, 1-week-old seedlings grown on vertical agar plates were immersed in 50 μg mL^{-1} propidium iodide for 30 min, washed twice with double-distilled water, and then observed. Staining was performed on two independent single insertion lines, showing consistent results.

SA Determination

Metabolites of pooled 5-week-old rosette leaves from four to six individual plants (snap-frozen in liquid nitrogen and stored at −80°C) were extracted with a 1+2 mixture of methanol and 2% (v/v) formic acid. The extract was split into three aliquots for separate determination of free SA, SA glucosides, and SA esters. For determination of the SA conjugates, the extract was digested overnight with β-glucosidase (Roth) or with esterase (Sigma-Aldrich). SA from undigested and digested samples was extracted under acidic conditions using reversed-phase sorbent cartridges (Oasis HLB 1 cc; Waters), recovered under basic conditions, and subsequently analyzed via HPLC. Quantification was based on SA fluorescence (excitation 305 nm/emission 400 nm) with *o*-anisic acid added as an internal standard during metabolite extraction and authentic SA standards. Thus, the content in free SA, in Glc-conjugated SA, and in esterified SA could be determined.

Nontargeted Metabolome Analysis

Three biological replicates and two technical replicates each were used for each genotype. Frozen root tissue was individually disrupted using a dismembrator. Metabolite extraction was performed as described previously (Weckwerth et al., 2004) with slight modifications. Loganin (44 μg mL^{-1}) and nitrophenol (3 μg mL^{-1}) were added to the extraction buffer (methanol/chloroform/water 2.5:1:1 [v/v/v]) as internal standards. After extraction, the aqueous phase was divided in several 200-μL aliquots and dried completely using a Speedvac. For FT-ICR MS analysis, one dried aliquot from each sample was redissolved in 70% methanol and diluted 1:25 in 70% methanol containing 35 pmol mL^{-1} dialanin.

Ultra-high-resolution mass spectra were acquired on a Bruker APEX Qe Fourier transform ion cyclotron resonance mass spectrometer (Bruker) equipped with a 12-T superconducting magnet and an APOLLO II electrospray ionization source. Measurements were performed in the negative ionization mode. Measurements in the positive ionization mode were also performed. However, in this case, there were no significant changes (at P value < 0.01), which were consistent in two independent knockout or overexpression lines, respectively. Samples were introduced into the electrospray source at a flow rate of 120 μL/h with a nebulizer gas pressure of 20 p.s.i. and a drying gas pressure of 15 p.s.i. (at 200°C). Spectra were externally calibrated based on Arg cluster ions (10 ppm). The spectra were acquired with a time domain of 1 megaword over a mass range between 146 and 2000 atomic mass units. Three hundred scans were accumulated for each spectrum. Internal mass calibration was performed using the internal standards (loganin and dialanin; Sigma-Aldrich) in addition to endogenous plant metabolites with calibration accuracy smaller than 0.01 ppm. Internal standards were also used to detect variation in the extraction procedure, matrix effects, and variation in the ionization efficiency in the electrospray source.

Mass lists were calibrated using the data analysis program (Bruker) and exported to ascii files. Mass list matrices for statistical analysis were produced using a custom-made program (M. Frommberger, Helmholtz Zentrum München). Masses, which were detected in only two or less out of six measurements in both genotypes, were deleted. Pearson correlation analysis (excluding missing values) was used to check extract reproducibility (correlation $r^2 > 0.9$). The sum of total peak intensities was monitored to detect variation in the ionization efficiency (in addition to internal standards). Nondetectable peaks were replaced by 200,000 counts, which were considered as the detection limit, to enable calculation of mean values and ratios. A two-sample Wilcoxon rank-sum test was performed for each mass separately to detect significant peak intensity differences between wild-type and mutant plants (detailed *m/z* lists are available in Supplemental Data Sets 1 and 2 online). The significance level was set to 1%. Measurements were repeated twice to filter for reproducible metabolites, and only those peaks were selected

that correlated with *UGT76B1* expression in both knockout and over-expression lines. Statistical analysis was performed in R (R Development Core Team, 2009).

Fragmentation Studies Using FT-ICR MS

For MS/MS fragmentation studies, the plant extract from *UGT76B1-OE-7* was partially cleaned and concentrated using a Strata NH_2 column (3 mL; Phenomenex). The targeted ions were trapped in a first hexapole for 200 ms prior to their mass selection inside a quadrupole mass filter. Once isolated, the targeted ions were accelerated and allowed to collide with argon atoms inside a second hexapole, which serves as a collision cell. The second hexapole had a relatively high pressure of 5×10^{-3} mbar. As a result of the collisions between the accelerated isolated ions and argon atoms in the second hexapole, product ions were produced and were forwarded to the ICR cell via a couple of accelerating and decelerating lenses. The ion accumulation time inside the collision cell was 500 ms.

For targeted ions with $m/z < 200$ amu, no quadrupole MS/MS fragmentation was done. Instead, the ions were forwarded as normal to the ICR cell and then they were isolated inside the cell by applying a frequency sweep to eject all ions but those that should be selected for further fragmentation events. Once isolated inside the ICR cell, the targeted ions could be excited in the radial plane, which was perpendicular to the magnetic field lines, by applying an on-resonance radial single-shot excitation pulse with a duration of 400 μs and a power of 4.5 Vp-p. A pulsed valve opened at the same time for 5 ms to inject argon atoms inside the ICR cell for collision-induced dissociation experiments. The produced fragment ions were then allowed to thermalize inside the cell before accelerating them in the radial plane for detection.

Recombinant UGT76B1 and Glucosyltransferase Assay

A glutathione *S*-transferase–UGT761 expression plasmid was constructed using pDEST15 (Invitrogen). The UGT76B1 open reading frame was amplified with the same primers as used for the construction of the overexpression lines. The recombinant protein was affinity purified using glutathione-coupled sepharose beads, according to the manufacturer's instructions (GE Healthcare), concentrated by membrane filtration (Amicon Ultra-4; Millipore) and supplemented with 20% glycerol for storage at −20°C (Messner et al., 2003).

To analyze the UGT enzyme activity assay, mixtures contained 0.1 M Tris–HCl, pH 7.5, 5 mM UDP-Glc, 0.5 mM aglycone, and ~1 μg fusion protein in a final volume of 50 μL. After incubation for 1 h at 30°C, the reaction was stopped by the addition of 200 μL methanol and cleared by centrifugation. Reactions were diluted 1:50 in 70% methanol (except for valic acid; see Supplemental Figure 13 online) and analyzed on an API4000 mass spectrometer using direct injection into the electrospray source at a flow rate of 30 μL. A total of 150 scans were accumulated for each measurement in the dual ion monitoring mode, which was adjusted to monitor ions at the nominal m/z ratios of the corresponding expected substrate and product peaks with a mass range of ±5 D.

ILA Treatment

For ILA treatment, 4-week-old plants were sprayed with 0.5 or 1 mM ILA (diluted in water) or only water for mock treatments. Plants were covered with a plexiglass lid until the surface of the leaves became dry. The fifth to eighth true leaves of each plant were harvested 24 h after treatment. Four leaves from three independent plants were pooled for each replicate and analyzed by real-time PCR.

Accession Numbers

Sequence data related to the genes described and analyzed in this article can be found in the Arabidopsis Genome Initiative or GenBank/EMBL databases under the following accession numbers: *UGT76B1* (At3g11340), *PR1* (At2g14610), *PDF1.2* (At5g44420), *VSP2* (At5g24770), *SAG13* (At2g29350), *SAG12* (At5g45890), *LOX2* (At3g45140), *WRKY70* (At3g56400), *EDS1* (At3g48090), *PAD4* (At3g52430), *JAR1* (At2g46370), *SID2* (At1g74710), *UBQ5* (At3g62250), and *S16* (At5g18380/At2g09990).

Supplemental Data

The following materials are available in the online version of this article.

Supplemental Figure 1. Molecular Characterization of *ugt76b1* Knockout and *UGT76B1* Overexpression Lines.

Supplemental Figure 2. Growth Phenotype of *ugt76b1* Knockout Mutants and the UGT76B1-OE-7 Overexpression Line.

Supplemental Figure 3. Early Senescence and Pathogen Resistance of *ugt76b1-2* Compared with L*er* (Wild-Type Background).

Supplemental Figure 4. Relative Quantification of *PR1* Expression at an Early Time Point.

Supplemental Figure 5. The Impact of *UGT76B1* Expression on the Onset of Senescence Is Dependent on *SID2* but Independent on *JAR1*.

Supplemental Figure 6. Detection of m/z 293.124 and 279.108 in Leaves of Col-0 and *UGT76B1-OE-7* Plants.

Supplemental Figure 7. Fragmentation Patterns of the Unknown Aglycon (Derived from m/z 293) from the Plant Extract and of Putative $C_6H_{12}O_3$ Isomers.

Supplemental Figure 8. In Vitro Activity Assay of UGT76B1 toward 2-Ethyl-2-Hydroxybutyric Acid.

Supplemental Figure 9. Isoleucic Acid Treatment in *ugt76b1-1* and *UGT76B1-OE-7*.

Supplemental Figure 10. *UGT76B1* Expression in Several Mutant Backgrounds.

Supplemental Figure 11. *ugt76b1-1* Knockout and *UGT76B1-OE-7* Plants Showed Inhibition of Root Growth on MeJA-Containing Medium Similar to Wild-Type Plants.

Supplemental Figure 12. Gene Network Suggesting a Relationship between *UGT76B1* and Branched-Chain Amino Acid Degradation Pathways.

Supplemental Figure 13. Valic Acid, a Putative Substrate of UGT76B1 in Addition to ILA.

Supplemental Table 1. Primer Pairs Used for qRT-PCR Analysis.

Supplemental Data Set 1. Nontargeted Metabolome Analyses of *ugt76b1* Knockout Lines versus Their Respective Wild Type.

Supplemental Data Set 2. Nontargeted Metabolome Analyses of *UGT76B1* Overexpression Lines versus Col-0.

provided access to an API4000 Q-Trap mass spectrometer. Lucia Gößl (Helmholtz Zentrum München) helped with the SA measurements. V.v.S.P. was supported by a Kekulé Fellowship of the Verband der Chemischen Industrie and W.Z. by a fellowship of the China Scholarship Council. Finally, we thank the three reviewers for their helpful comments, which improved the manuscript.

AUTHOR CONTRIBUTIONS

REFERENCES

Balagué, C., Lin, B., Alcon, C., Flottes, G., Malmström, S., Köhler, C., Neuhaus, G., Pelletier, G., Gaymard, F., and Roby, D. (2003). HLM1, an essential signaling component in the hypersensitive response, is a member of the cyclic nucleotide-gated channel ion channel family. Plant Cell **15:** 365–379.

Bandu, M.L., Grubbs, T., Kater, M., and Desaire, H. (2006). Collision induced dissociation of alpha hydroxy acids: Evidence of an ion-neutral complex intermediate. Int. J. Mass Spectrom. **251:** 40–46.

Barth, C., Moeder, W., Klessig, D.F., and Conklin, P.L. (2004). The timing of senescence and response to pathogens is altered in the ascorbate-deficient Arabidopsis mutant vitamin c-1. Plant Physiol. **134:** 1784–1792.

Battke, F., Schramel, P., and Ernst, D. (2003). A novel method for in vitro culture of plants: Cultivation of barley in a floating hydroponic system. Plant Mol. Biol. Rep. **21:** 405–409.

Bensmihen, S., To, A., Lambert, G., Kroj, T., Giraudat, J., and Parcy, F. (2004). Analysis of an activated ABI5 allele using a new selection method for transgenic *Arabidopsis* seeds. FEBS Lett. **561:** 127–131.

Berger, S. (2002). Jasmonate-related mutants of *Arabidopsis* as tools for studying stress signaling. Planta **214:** 497–504.

Binder, S., Knill, T., and Schuster, J. (2007). Branched-chain amino acid metabolism in higher plants. Physiol. Plant. **129:** 68–78.

Blanco, F., Salinas, P., Cecchini, N.M., Jordana, X., Van Hummelen, P., Alvarez, M.E., and Holuigue, L. (2009). Early genomic responses to salicylic acid in *Arabidopsis*. Plant Mol. Biol. **70:** 79–102.

Bolton, M.D. (2009). Primary metabolism and plant defense—Fuel for the fire. Mol. Plant Microbe Interact. **22:** 487–497.

Bowles, D., Isayenkova, J., Lim, E.K., and Poppenberger, B. (2005). Glycosyltransferases: Managers of small molecules. Curr. Opin. Plant Biol. **8:** 254–263.

Bowles, D., Lim, E.K., Poppenberger, B., and Vaistij, F.E. (2006). Glycosyltransferases of lipophilic small molecules. Annu. Rev. Plant Biol. **57:** 567–597.

Bowling, S.A., Clarke, J.D., Liu, Y., Klessig, D.F., and Dong, X. (1997). The *cpr5* mutant of *Arabidopsis* expresses both NPR1-dependent and NPR1-independent resistance. Plant Cell **9:** 1573–1584.

Bowling, S.A., Guo, A., Cao, H., Gordon, A.S., Klessig, D.F., and Dong, X. (1994). A mutation in *Arabidopsis* that leads to constitutive expression of systemic acquired resistance. Plant Cell **6:** 1845–1857.

Brazier-Hicks, M., and Edwards, R. (2005). Functional importance of the family 1 glucosyltransferase *UGT72B1* in the metabolism of xenobiotics in *Arabidopsis thaliana*. Plant J. **42:** 556–566.

Brodersen, P., Petersen, M., Bjørn Nielsen, H., Zhu, S., Newman, M.A., Shokat, K.M., Rietz, S., Parker, J., and Mundy, J. (2006). *Arabidopsis* MAP kinase 4 regulates salicylic acid- and jasmonic acid/ethylene-dependent responses via EDS1 and PAD4. Plant J. **47:** 532–546.

Buchanan-Wollaston, V., Page, T., Harrison, E., Breeze, E., Lim, P.O., Nam, H.G., Lin, J.F., Wu, S.H., Swidzinski, J., Ishizaki, K., and Leaver, C.J. (2005). Comparative transcriptome analysis reveals significant differences in gene expression and signalling pathways between developmental and dark/starvation-induced senescence in *Arabidopsis*. Plant J. **42:** 567–585.

Caille, S., Cui, S., Hwang, T.L., Wang, X., and Faul, M.M. (2009). Two asymmetric syntheses of AMG 221, an inhibitor of 11beta-hydroxysteroid dehydrogenase type 1. J. Org. Chem. **74:** 3833–3842.

Clough, S.J., and Bent, A.F. (1998). Floral dip: A simplified method for *Agrobacterium*-mediated transformation of *Arabidopsis thaliana*. Plant J. **16:** 735–743.

Consonni, C., Humphry, M.E., Hartmann, H.A., Livaja, M., Durner, J., Westphal, L., Vogel, J., Lipka, V., Kemmerling, B., Schulze-Lefert, P., Somerville, S.C., and Panstruga, R. (2006). Conserved requirement for a plant host cell protein in powdery mildew pathogenesis. Nat. Genet. **38:** 716–720.

Dean, J.V., and Delaney, S.P. (2008). Metabolism of salicylic acid in wild-type, *ugt74f1* and *ugt74f2* glucosyltransferase mutants of *Arabidopsis thaliana*. Physiol. Plant. **132:** 417–425.

Devadas, S.K., Enyedi, A., and Raina, R. (2002). The *Arabidopsis hrl1* mutation reveals novel overlapping roles for salicylic acid, jasmonic acid and ethylene signalling in cell death and defence against pathogens. Plant J. **30:** 467–480.

Feys, B.J., Moisan, L.J., Newman, M.A., and Parker, J.E. (2001). Direct interaction between the *Arabidopsis* disease resistance signaling proteins, EDS1 and PAD4. EMBO J. **20:** 5400–5411.

Fonseca, S., Chini, A., Hamberg, M., Adie, B., Porzel, A., Kramell, R., Miersch, O., Wasternack, C., and Solano, R. (2009). (+)-7-Iso-jasmonoyl-L-isoleucine is the endogenous bioactive jasmonate. Nat. Chem. Biol. **5:** 344–350.

Fridman, E., and Pichersky, E. (2005). Metabolomics, genomics, proteomics, and the identification of enzymes and their substrates and products. Curr. Opin. Plant Biol. **8:** 242–248.

Gachon, C.M.M., Langlois-Meurinne, M., and Saindrenan, P. (2005). Plant secondary metabolism glycosyltransferases: The emerging functional analysis. Trends Plant Sci. **10:** 542–549.

Gaffney, T., Friedrich, L., Vernooij, B., Negrotto, D., Nye, G., Uknes, S., Ward, E., Kessmann, H., and Ryals, J. (1993). Requirement of salicylic acid for the induction of systemic acquired resistance. Science **261:** 754–756.

Genger, R.K., Jurkowski, G.I., McDowell, J.M., Lu, H., Jung, H.W., Greenberg, J.T., and Bent, A.F. (2008). Signaling pathways that regulate the enhanced disease resistance of *Arabidopsis* "defense, no death" mutants. Mol. Plant Microbe Interact. **21:** 1285–1296.

Glazebrook, J. (2005). Contrasting mechanisms of defense against biotrophic and necrotrophic pathogens. Annu. Rev. Phytopathol. **43:** 205–227.

Glazebrook, J., Rogers, E.E., and Ausubel, F.M. (1996). Isolation of *Arabidopsis* mutants with enhanced disease susceptibility by direct screening. Genetics **143:** 973–982.

Gou, M., Su, N., Zheng, J., Huai, J., Wu, G., Zhao, J., He, J., Tang, D., Yang, S., and Wang, G. (2009). An F-box gene, *CPR30*, functions as a negative regulator of the defense response in *Arabidopsis*. Plant J. **60:** 757–770.

Greenberg, J.T., Guo, A., Klessig, D.F., and Ausubel, F.M. (1994).

Programmed cell death in plants: A pathogen-triggered response activated coordinately with multiple defense functions. Cell **77:** 551–563.

Grubb, C.D., Zipp, B.J., Ludwig-Müller, J., Masuno, M.N., Molinski, T.F., and Abel, S. (2004). *Arabidopsis* glucosyltransferase UGT74B1 functions in glucosinolate biosynthesis and auxin homeostasis. Plant J. **40:** 893–908.

Hanson, A.D., Pribat, A., Waller, J.C., and de Crecy-Lagard, V. (2010). 'Unknown' proteins and 'orphan' enzymes: The missing half of the engineering parts list–and how to find it. Biochem. J. **425:** 1–11.

Heidel, A.J., Clarke, J.D., Antonovics, J., and Dong, X.N. (2004). Fitness costs of mutations affecting the systemic acquired resistance pathway in *Arabidopsis thaliana*. Genetics **168:** 2197–2206.

Heil, M., and Baldwin, I.T. (2002). Fitness costs of induced resistance: Emerging experimental support for a slippery concept. Trends Plant Sci. **7:** 61–67.

Hirai, M.Y., et al. (2005). Elucidation of gene-to-gene and metabolite-to-gene networks in *Arabidopsis* by integration of metabolomics and transcriptomics. J. Biol. Chem. **280:** 25590–25595.

Hugouvieux, V., Barber, C.E., and Daniels, M.J. (1998). Entry of *Xanthomonas campestris* pv. *campestris* into hydathodes of *Arabidopsis thaliana* leaves: A system for studying early infection events in bacterial pathogenesis. Mol. Plant Microbe Interact. **11:** 537–543.

Jackson, R.G., Kowalczyk, M., Li, Y., Higgins, G., Ross, J., Sandberg, G., and Bowles, D.J. (2002). Over-expression of an *Arabidopsis* gene encoding a glucosyltransferase of indole-3-acetic acid: Phenotypic characterisation of transgenic lines. Plant J. **32:** 573–583.

Jackson, R.G., Lim, E.K., Li, Y., Kowalczyk, M., Sandberg, G., Hoggett, J., Ashford, D.A., and Bowles, D.J. (2001). Identification and biochemical characterization of an *Arabidopsis* indole-3-acetic acid glucosyltransferase. J. Biol. Chem. **276:** 4350–4356.

Jones, J.D., and Dangl, J.L. (2006). The plant immune system. Nature **444:** 323–329.

Jones, P., Messner, B., Nakajima, J., Schäffner, A.R., and Saito, K. (2003). UGT73C6 and UGT78D1, glycosyltransferases involved in flavonol glycoside biosynthesis in *Arabidopsis thaliana*. J. Biol. Chem. **278:** 43910–43918.

Jones, P., and Vogt, T. (2001). Glycosyltransferases in secondary plant metabolism: Tranquilizers and stimulant controllers. Planta **213:** 164–174.

Journot-Catalino, N., Somssich, I.E., Roby, D., and Kroj, T. (2006). The transcription factors WRKY11 and WRKY17 act as negative regulators of basal resistance in *Arabidopsis thaliana*. Plant Cell **18:** 3289–3302.

Karimi, M., Inzé, D., and Depicker, A. (2002). GATEWAY vectors for Agrobacterium-mediated plant transformation. Trends Plant Sci. **7:** 193–195.

Katagiri, F., Thilmony, R., and He, S. (2002). The *Arabidopsis thaliana*–*Pseudomonas syringae* interaction. In The Arabidopsis Book **1:** e0039, doi/10.1199/tab.0039.

Katari, M.S., Nowicki, S.D., Aceituno, F.F., Nero, D., Kelfer, J., Thompson, L.P., Cabello, J.M., Davidson, R.S., Goldberg, A.P., Shasha, D.E., Coruzzi, G.M., and Gutiérrez, R.A. (2010). VirtualPlant: A software platform to support systems biology research. Plant Physiol. **152:** 500–515.

Kazan, K., and Manners, J.M. (2008). Jasmonate signaling: Toward an integrated view. Plant Physiol. **146:** 1459–1468.

Kloek, A.P., Verbsky, M.L., Sharma, S.B., Schoelz, J.E., Vogel, J., Klessig, D.F., and Kunkel, B.N. (2001). Resistance to *Pseudomonas syringae* conferred by an *Arabidopsis thaliana* coronatine-insensitive (coi1) mutation occurs through two distinct mechanisms. Plant J. **26:** 509–522.

Konieczny, A., and Ausubel, F.M. (1993). A procedure for mapping *Arabidopsis* mutations using co-dominant ecotype-specific PCR-based markers. Plant J. **4:** 403–410.

Koornneef, A., Leon-Reyes, A., Ritsema, T., Verhage, A., Den Otter, F.C., Van Loon, L.C., and Pieterse, C.M. (2008). Kinetics of salicylate-mediated suppression of jasmonate signaling reveal a role for redox modulation. Plant Physiol. **147:** 1358–1368.

Koornneef, A., and Pieterse, C.M. (2008). Cross talk in defense signaling. Plant Physiol. **146:** 839–844.

Kus, J.V., Zaton, K., Sarkar, R., and Cameron, R.K. (2002). Age-related resistance in *Arabidopsis* is a developmentally regulated defense response to *Pseudomonas syringae*. Plant Cell **14:** 479–490.

Lagarde, D., Basset, M., Lepetit, M., Conejero, G., Gaymard, F., Astruc, S., and Grignon, C. (1996). Tissue-specific expression of *Arabidopsis AKT1* gene is consistent with a role in K+ nutrition. Plant J. **9:** 195–203.

Langlois-Meurinne, M., Gachon, C.M.M., and Saindrenan, P. (2005). Pathogen-responsive expression of glycosyltransferase genes *UGT73B3* and *UGT73B5* is necessary for resistance to *Pseudomonas syringae* pv *tomato* in Arabidopsis. Plant Physiol. **139:** 1890–1901.

Li, J., Brader, G., and Palva, E.T. (2004). The WRKY70 transcription factor: A node of convergence for jasmonate-mediated and salicylate-mediated signals in plant defense. Plant Cell **16:** 319–331.

Li, X., Zhang, Y., Clarke, J.D., Li, Y., and Dong, X. (1999). Identification and cloning of a negative regulator of systemic acquired resistance, SNI1, through a screen for suppressors of *npr1-1*. Cell **98:** 329–339.

Li, Y., Baldauf, S., Lim, E.K., and Bowles, D.J. (2001). Phylogenetic analysis of the UDP-glycosyltransferase multigene family of *Arabidopsis thaliana*. J. Biol. Chem. **276:** 4338–4343.

Lim, E.K., Doucet, C.J., Hou, B., Jackson, R.G., Abrams, S.R., and Bowles, D.J. (2005). Resolution of (+)-abscisic acid using an *Arabidopsis* glycosyltransferase. Tetrahedron Asymmetry **16:** 143–147.

Lim, E.K., Doucet, C.J., Li, Y., Elias, L., Worrall, D., Spencer, S.P., Ross, J., and Bowles, D.J. (2002). The activity of *Arabidopsis* glycosyltransferases toward salicylic acid, 4-hydroxybenzoic acid, and other benzoates. J. Biol. Chem. **277:** 586–592.

Lorrain, S., Vailleau, F., Balagué, C., and Roby, D. (2003). Lesion mimic mutants: Keys for deciphering cell death and defense pathways in plants? Trends Plant Sci. **8:** 263–271.

Mackenzie, P.I., et al. (1997). The UDP glycosyltransferase gene superfamily: Recommended nomenclature update based on evolutionary divergence. Pharmacogenetics **7:** 255–269.

Mamer, O.A., and Reimer, M.L. (1992). On the mechanisms of the formation of L-alloisoleucine and the 2-hydroxy-3-methylvaleric acid stereoisomers from L-isoleucine in maple syrup urine disease patients and in normal humans. J. Biol. Chem. **267:** 22141–22147.

Matsuda, F., Yonekura-Sakakibara, K., Niida, R., Kuromori, T., Shinozaki, K., and Saito, K. (2009). MS/MS spectral tag-based annotation of non-targeted profile of plant secondary metabolites. Plant J. **57:** 555–577.

Messner, B., Thulke, O., and Schäffner, A.R. (2003). *Arabidopsis* glucosyltransferases with activities toward both endogenous and xenobiotic substrates. Planta **217:** 138–146.

Miao, Y., and Zentgraf, U. (2007). The antagonist function of *Arabidopsis* WRKY53 and ESR/ESP in leaf senescence is modulated by the jasmonic and salicylic acid equilibrium. Plant Cell **19:** 819–830.

Morris, K., MacKerness, S.A.H., Page, T., John, C.F., Murphy, A.M., Carr, J.P., and Buchanan-Wollaston, V. (2000). Salicylic acid has a role in regulating gene expression during leaf senescence. Plant J. **23:** 677–685.

Mur, L.A.J., Kenton, P., Atzorn, R., Miersch, O., and Wasternack, C. (2006). The outcomes of concentration-specific interactions between

salicylate and jasmonate signaling include synergy, antagonism, and oxidative stress leading to cell death. Plant Physiol. **140:** 249–262.

Nawrath, C., and Métraux, J.P. (1999). Salicylic acid induction-deficient mutants of *Arabidopsis* express PR-2 and PR-5 and accumulate high levels of camalexin after pathogen inoculation. Plant Cell **11:** 1393–1404.

Obayashi, T., Hayashi, S., Saeki, M., Ohta, H., and Kinoshita, K. (2009). ATTED-II provides coexpressed gene networks for *Arabidopsis*. Nucleic Acids Res. **37**(Database issue): D987–D991.

Oh, S.A., Lee, S.Y., Chung, I.K., Lee, C.H., and Nam, H.G. (1996). A senescence-associated gene of *Arabidopsis thaliana* is distinctively regulated during natural and artificially induced leaf senescence. Plant Mol. Biol. **30:** 739–754.

Ohta, D., Kanaya, S., and Suzuki, H. (2010). Application of Fourier-transform ion cyclotron resonance mass spectrometry to metabolic profiling and metabolite identification. Curr. Opin. Biotechnol. **21:** 35–44.

Park, J.E., Park, J.Y., Kim, Y.S., Staswick, P.E., Jeon, J., Yun, J., Kim, S.Y., Kim, J., Lee, Y.H., and Park, C.M. (2007). GH3-mediated auxin homeostasis links growth regulation with stress adaptation response in *Arabidopsis*. J. Biol. Chem. **282:** 10036–10046.

Petersen, M., et al. (2000). *Arabidopsis* map kinase 4 negatively regulates systemic acquired resistance. Cell **103:** 1111–1120.

Pieterse, C.M., Leon-Reyes, A., Van der Ent, S., and Van Wees, S.C. (2009). Networking by small-molecule hormones in plant immunity. Nat. Chem. Biol. **5:** 308–316.

Pinheiro, J., Bates, D., DebRoy, S., Sarkar, D., and the R Development Core Team. (2009). nlme: Linear and Nonlinear Mixed Effects Models. R package version 3.1–94.

Pitzschke, A., Djamei, A., Bitton, F., and Hirt, H. (2009). A major role of the MEKK1-MKK1/2-MPK4 pathway in ROS signalling. Mol. Plant **2:** 120–137.

Podebrad, F., Heil, M., Leib, S., Geier, B., Beck, T., Mosandl, A., Sewell, A.C., and Bohles, H. (1997). Analytical approach in diagnosis of inherited metabolic diseases: Maple syrup urine disease (MSUD) - Simultaneous analysis of metabolites in urine by enantioselective multidimensional capillary gas chromatography mass spectrometry (enantio-MDGC-MS). J. High Resolut. Chromatogr. **20:** 355–362.

Pogány, M., von Rad, U., Grün, S., Dongó, A., Pintye, A., Simoneau, P., Bahnweg, G., Kiss, L., Barna, B., and Durner, J. (2009). Dual roles of reactive oxygen species and NADPH oxidase RBOHD in an *Arabidopsis-Alternaria* pathosystem. Plant Physiol. **151:** 1459–1475.

Poppenberger, B., Fujioka, S., Soeno, K., George, G.L., Vaistij, F.E., Hiranuma, S., Seto, H., Takatsuto, S., Adam, G., Yoshida, S., and Bowles, D. (2005). The UGT73C5 of *Arabidopsis thaliana* glucosylates brassinosteroids. Proc. Natl. Acad. Sci. USA **102:** 15253–15258.

Quirino, B.F., Normanly, J., and Amasino, R.M. (1999). Diverse range of gene activity during *Arabidopsis thaliana* leaf senescence includes pathogen-independent induction of defense-related genes. Plant Mol. Biol. **40:** 267–278.

R Development Core Team (2009). R: A Language and Environment for Statistical Computing. (Vienna, Austria: R Foundation for Statistical Computing).

Rieu, I., and Powers, S.J. (2009). Real-time quantitative RT-PCR: Design, calculations, and statistics. Plant Cell **21:** 1031–1033.

Ross, J., Li, Y., Lim, E., and Bowles, D.J. (2001). Higher plant glycosyltransferases. Genome Biol. **2:** REVIEWS3004.

Rustérucci, C., Aviv, D.H., Holt III, B.F., Dangl, J.L., and Parker, J.E. (2001). The disease resistance signaling components EDS1 and PAD4 are essential regulators of the cell death pathway controlled by LSD1 in *Arabidopsis*. Plant Cell **13:** 2211–2224.

Saito, K., Hirai, M.Y., and Yonekura-Sakakibara, K. (2008). Decoding

genes with coexpression networks and metabolomics - 'majority report by precogs'. Trends Plant Sci. **13:** 36–43.

Sasaki, Y., et al. (2001). Monitoring of methyl jasmonate-responsive genes in *Arabidopsis* by cDNA macroarray: Self-activation of jasmonic acid biosynthesis and crosstalk with other phytohormone signaling pathways. DNA Res. **8:** 153–161.

Scholl, R.L., May, S.T., and Ware, D.H. (2000). Seed and molecular resources for *Arabidopsis*. Plant Physiol. **124:** 1477–1480.

Shah, J., Kachroo, P., and Klessig, D.F. (1999). The *Arabidopsis ssi1* mutation restores pathogenesis-related gene expression in *npr1* plants and renders defensin gene expression salicylic acid dependent. Plant Cell **11:** 191–206.

Silva, H., Yoshioka, K., Dooner, H.K., and Klessig, D.F. (1999). Characterization of a new *Arabidopsis* mutant exhibiting enhanced disease resistance. Mol. Plant Microbe Interact. **12:** 1053–1063.

Song, J.T., Koo, Y.J., Seo, H.S., Kim, M.C., Choi, Y.D., and Kim, J.H. (2008). Overexpression of AtSGT1, an *Arabidopsis* salicylic acid glucosyltransferase, leads to increased susceptibility to *Pseudomonas syringae*. Phytochemistry **69:** 1128–1134.

Song, J.T., Lu, H., and Greenberg, J.T. (2004). Divergent roles in *Arabidopsis thaliana* development and defense of two homologous genes, *aberrant growth and death2* and *AGD2-LIKE DEFENSE RESPONSE PROTEIN1*, encoding novel aminotransferases. Plant Cell **16:** 353–366.

Spoel, S.H., Johnson, J.S., and Dong, X. (2007). Regulation of trade-offs between plant defenses against pathogens with different life-styles. Proc. Natl. Acad. Sci. USA **104:** 18842–18847.

Spoel, S.H., et al. (2003). NPR1 modulates cross-talk between salicylate- and jasmonate-dependent defense pathways through a novel function in the cytosol. Plant Cell **15:** 760–770.

Sprague, S.J., Watt, M., Kirkegaard, J.A., and Howlett, B.J. (2007). Pathways of infection of *Brassica napus* roots by *Leptosphaeria maculans*. New Phytol. **176:** 211–222.

Staswick, P.E., and Tiryaki, I. (2004). The oxylipin signal jasmonic acid is activated by an enzyme that conjugates it to isoleucine in *Arabidopsis*. Plant Cell **16:** 2117–2127.

Tohge, T., et al. (2005). Functional genomics by integrated analysis of metabolome and transcriptome of *Arabidopsis* plants over-expressing an MYB transcription factor. Plant J. **42:** 218–235.

Toufighi, K., Brady, S.M., Austin, R., Ly, E., and Provart, N.J. (2005). The Botany Array Resource: e-Northerns, expression angling, and promoter analyses. Plant J. **43:** 153–163.

Uknes, S., Mauch-Mani, B., Moyer, M., Potter, S., Williams, S., Dincher, S., Chandler, D., Slusarenko, A., Ward, E., and Ryals, J. (1992). Acquired resistance in *Arabidopsis*. Plant Cell **4:** 645–656.

Ülker, B., Shahid Mukhtar, M., and Somssich, I.E. (2007). The WRKY70 transcription factor of *Arabidopsis* influences both the plant senescence and defense signaling pathways. Planta **226:** 125–137.

Vandesompele, J., De Preter, K., Pattyn, F., Poppe, B., Van Roy, N., De Paepe, A., and Speleman, F. (2002). Accurate normalization of real-time quantitative RT-PCR data by geometric averaging of multiple internal control genes. Genome Biol. **3:** RESEARCH0034.

Vlot, A.C., Dempsey, D.A., and Klessig, D.F. (2009). Salicylic acid, a multifaceted hormone to combat disease. Annu. Rev. Phytopathol. **47:** 177–206.

Vogt, T., and Jones, P. (2000). Glycosyltransferases in plant natural product synthesis: Characterization of a supergene family. Trends Plant Sci. **5:** 380–386.

Weaver, L.M., Gan, S., Quirino, B., and Amasino, R.M. (1998). A comparison of the expression patterns of several senescence-associated genes in response to stress and hormone treatment. Plant Mol. Biol. **37:** 455–469.

Weckwerth, W., Wenzel, K., and Fiehn, O. (2004). Process for the

integrated extraction, identification and quantification of metabolites, proteins and RNA to reveal their co-regulation in biochemical networks. Proteomics **4:** 78–83.

Wildermuth, M.C., Dewdney, J., Wu, G., and Ausubel, F.M. (2001). Isochorismate synthase is required to synthesize salicylic acid for plant defence. Nature **414:** 562–565.

Yabuuchi, T., and Kusumi, T. (1999). A convenient one-pot synthesis of quaternary alpha-methoxy- and alpha-hydroxycarboxylic acids. Chem. Pharm. Bull. (Tokyo) **47:** 684–686.

Yonekura-Sakakibara, K., Tohge, T., Matsuda, F., Nakabayashi, R., Takayama, H., Niida, R., Watanabe-Takahashi, A., Inoue, E., and Saito, K. (2008). Comprehensive flavonol profiling and transcriptome

coexpression analysis leading to decoding gene-metabolite correlations in *Arabidopsis*. Plant Cell **20:** 2160–2176.

Yoshida, S., Ito, M., Nishida, I., and Watanabe, A. (2002). Identification of a novel gene HYS1/CPR5 that has a repressive role in the induction of leaf senescence and pathogen-defence responses in *Arabidopsis thaliana*. Plant J. **29:** 427–437.

Zhou, N., Tootle, T.L., Tsui, F., Klessig, D.F., and Glazebrook, J. (1998). *PAD4* functions upstream from salicylic acid to control defense responses in *Arabidopsis*. Plant Cell **10:** 1021–1030.

Zimmermann, P., Hennig, L., and Gruissem, W. (2005). Gene-expression analysis and network discovery using Genevestigator. Trends Plant Sci. **10:** 407–409.